Accepted Manuscript

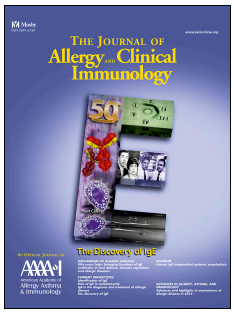

Human NLRP3 inflammasome activity is regulated by and potentially targetable via BTK

Xiao Liu, MSc, Tica Pichulik, PhD MSc, Olaf-Oliver Wolz, PhD Dipl Biol, Truong-Minh Dang, PhD MSc, Andrea Stutz, MSc, Carly Dillen, PhD MSc, Magno Delmiro Garcia, MSc, Helene Kraus, MD, Sabine Dickhöfer, MTA, Ellen Daiber, Dipl Biol, Lisa Münzenmayer, MSc, Silke Wahl, PhD MSc, Nikolaus Rieber, MD, Jasmin Kümmerle-Deschner, MD, Amir Yazdi, MD, Mirita Franz-Wachtel, PhD MSc, Boris Macek, PhD MSc, Markus Radsak, MD, Sebastian Vogel, MD, Berit Schulte, MD, Juliane Sarah Walz, MD, Dominik Hartl, Prof. PhD MD, Eicke Latz, Prof. PhD MD, Stephan Stilgenbauer, Prof. PhD MD, Bodo Grimbacher, Prof. PhD MD, Lloyd Miller, PhD MD, Cornelia Brunner, Prof. PhD MSc, Christiane Wolz, Prof. PhD MSc, Alexander N.R. Weber, Prof. PhD MPhil

PII: S0091-6749(17)30232-4

DOI: 10.1016/j.jaci.2017.01.017

Reference: YMAI 12641

To appear in: *Journal of Allergy and Clinical Immunology*

Received Date: 8 April 2016

Revised Date: 23 December 2016

Accepted Date: 11 January 2017

Please cite this article as: Liu X, Pichulik T, Wolz O-O, Dang T-M, Stutz A, Dillen C, Delmiro Garcia M, Kraus H, Dickhöfer S, Daiber E, Münzenmayer L, Wahl S, Rieber N, Kümmerle-Deschner J, Yazdi A, Franz-Wachtel M, Macek B, Radsak M, Vogel S, Schulte B, Walz JS, Hartl D, Latz E, Stilgenbauer S, Grimbacher B, Miller L, Brunner C, Wolz C, Weber ANR, Human NLRP3 inflammasome activity is regulated by and potentially targetable via BTK, *Journal of Allergy and Clinical Immunology* (2017), doi: 10.1016/j.jaci.2017.01.017.

This is a PDF file of an unedited manuscript that has been accepted for publication. As a service to our customers we are providing this early version of the manuscript. The manuscript will undergo copyediting, typesetting, and review of the resulting proof before it is published in its final form. Please

note that during the production process errors may be discovered which could affect the content, and all legal disclaimers that apply to the journal pertain.

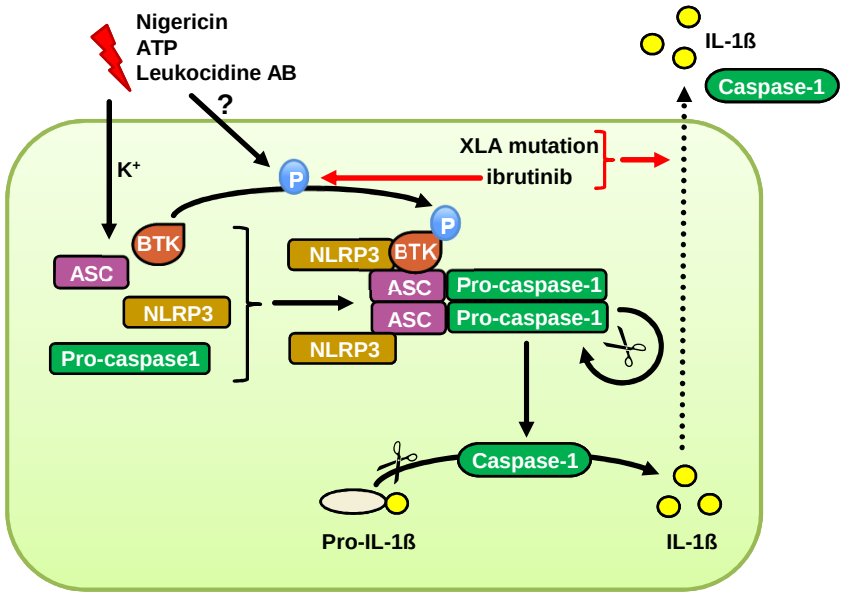
Nigericin
ATP
Leukocidine AB
?
K+
P
XLA mutation
ibrutinib
IL-1ß
Caspase-1
BTK
ASC
NLRP3
Pro-caspase1
P
NLRP3
BTK
ASC
Pro-caspase-1
ASC
Pro-caspase-1
NLRP3
Caspase-1
Pro-IL-1ß
IL-1ß

ACCEPTED MANUSCRIPT

Title

Human NLRP3 inflammasome activity is regulated by and potentially targetable via BTK

Authors

Xiao Liu[a] MSc, Tica Pichulik[a] PhD MSc, Olaf-Oliver Wolz[a] PhD Dipl Biol, Truong-Minh Dang[a] PhD MSc, Andrea Stutz[b] MSc, Carly Dillen[c] PhD MSc, Magno Delmiro Garcia[a] MSc, Helene Kraus[d] MD, Sabine Dickhöfer[a] MTA, Ellen Daiber[e] Dipl Biol, Lisa Münzenmayer[e] MSc, Silke Wahl[f] PhD MSc, Nikolaus Rieber[g] MD, Jasmin Kümmerle-Deschner[g] MD, Amir Yazdi[h] MD, Mirita Franz-Wachtel[f] PhD MSc, Boris Macek[f] PhD MSc, Markus Radsak[i] MD, Sebastian Vogel[j] MD, Berit Schulte[e] MD, Juliane Sarah Walz[k] MD, Dominik Hartl[g] Prof. PhD MD, Eicke Latz[b,l] Prof. PhD MD, Stephan Stilgenbauer[m] Prof. PhD MD, Bodo Grimbacher[d] Prof. PhD MD, Lloyd Miller[c] PhD MD, Cornelia Brunner[n] Prof. PhD MSc, Christiane Wolz[e] Prof. PhD MSc, Alexander N. R. Weber[a]* Prof. PhD MPhil

Affiliations

[a] Interfaculty Institute for Cell Biology, Department of Immunology, University of Tübingen, Auf der Morgenstelle 15, 72076 Tübingen, Germany

[b] Institute of Innate Immunity, University Hospital Bonn, Sigmund-Freud-Str. 25, 53127 Bonn, Germany.

[c] Department of Dermatology, Johns Hopkins University, 1550 Orleans St, Baltimore, MD 21231, USA

[d] Centre of Chronic Immunodeficiency, University Hospital Freiburg, Engesserstr. 4, 79108 Freiburg, Germany

[e] Interfaculty Institute of Microbiology and Infection Medicine, University of Tübingen, Elfriede-Aulhorn-Str. 6, 72076 Tübingen, Germany

[f] Proteome Center Tübingen, University of Tübingen, Auf der Morgenstelle 15, 72076 Tübingen, Germany

ACCEPTED MANUSCRIPT

25 [g] Department of Pediatrics I, University Hospital Tübingen, Hoppe-Seyler-Str. 1, 72076 Tübingen,
26 Germany

27 [h] Department of Dermatology, University Hospital Tübingen, Liebermeisterstr. 25, 72076 Tübingen,
28 Germany

29 [i] Medical Hospital III, University Hospital Mainz, Langenbeckstr. 1, 55101 Mainz, Germany

30 [j] Department of Cardiology and Cardiovascular Diseases, University Hospital Tübingen, Otfried-
31 Müller-Str. 10, 72076 Tübingen, Germany

32 [k] Medical Hospital II (Department of Hematology and Oncology), University Hospital Tübingen,
33 Otfried-Müller-Str. 10, 72076 Tübingen, Germany

34 [l] Division of Infectious Diseases & Immunology, University of Massachusetts, 364 Plantation St,
35 Worcester, MA 01605, USA

36 [m] Department of Internal Medicine III, Ulm University Hospital, Albert-Einstein-Allee 23, 89081 Ulm,
37 Germany

38 [n] Department of Otorhinolaryngology, Ulm University Medical Center, Frauensteige 14a, 89075 Ulm,
39 Germany

40

41 **Contact information**

42 * to whom correspondence should be addressed: Alexander Weber; Interfaculty Institute for Cell
43 Biology, Department of Immunology, University of Tübingen, Auf der Morgenstelle 15, 72076
44 Tübingen, Germany; Tel. +49 7071 2987623; Fax. +49 7071 294759;
45 alexander.weber@uni.tuebingen.de

46

47 **Funding**

ACCEPTED MANUSCRIPT

48 The study was supported by the Else-Kröner-Fresenius Stiftung (to ANRW), the University of
49 Tübingen and the University Hospital Tübingen (Fortüne Grant 2310-0-0 to XL and ANRW).

ACCEPTED MANUSCRIPT

ACCEPTED MANUSCRIPT

Abstract

Background: The Nod-like receptor, NACHT, LRR and PYD domains-containing protein 3 (NLRP3), and Bruton's tyrosine kinase (BTK) are protagonists in innate and adaptive immunity, respectively: NLRP3 senses exogenous and endogenous insults leading to inflammasome activation, which occurs spontaneously in Muckle-Wells Syndrome (MWS); *BTK* mutations cause the genetic immunodeficiency X-linked agammaglobulinemia (XLA). However, to date few proteins that regulate NLRP3 inflammasome activity in human primary immune cells have been identified and clinically promising pharmacological targeting strategies remain elusive.

Objective: We therefore sought to identify novel regulators of the NLRP3 inflammasome in human cells with a view to exploring interference with inflammasome activity at the level of such regulators.

Methods: Following proteome-wide phospho-proteomics, an identified novel regulator, BTK, was studied in human and murine cells using pharmacological and genetic BTK ablation.

Results: We here show that BTK is a critical regulator of NLRP3 inflammasome activation: Pharmacological (using the Food and Drug Administration (FDA)-approved inhibitor, ibrutinib) and genetic (in XLA patients and *Btk*-knockout mice) BTK ablation in primary immune cells led to reduced Interleukin (IL)-1β processing and secretion in response to Nigericin and the *Staphylococcus aureus* toxin, Leukocidin (Luk) AB. BTK affected Apoptosis-associated speck-like protein containing a CARD (ASC) speck formation and caspase-1 cleavage and interacted with NLRP3 and ASC. *S. aureus* infection control *in vivo* and IL-1β release from MWS patient cells were impaired by ibrutinib. Notably, IL-1β processing and release from immune cells isolated from cancer patients on ibrutinib therapy was reduced.

Conclusion: Our data suggest that XLA may partially result from genetic inflammasome deficiency and that NLRP3 inflammasome-linked inflammation could potentially be targeted pharmacologically via BTK.

ACCEPTED MANUSCRIPT

74 **Clinical implications**

75 Based on our results it could be speculated that the NLRP3 inflammasome, which contributes to
76 inflammatory pathologies in humans, could potentially be targeted using BTK inhibitors.

77 **Capsule summary**

78 We show a critical and potentially therapeutically tractable role for BTK in NLRP3 inflammasome
79 regulation in human primary cells.

80 **Keywords**

81 Interleukin-1, ibrutinib, Bruton's Tyrosine Kinase, NLRP3, Inflammasome, Macrophage, X-linked
82 agammaglobulinemia, Staphylococcus aureus, Muckle-Wells Syndrome, Inflammation.

83 **Abbreviations**

84 ASC – Apoptosis-associated speck-like protein containing a CARD; BTK – Bruton's Tyrosine Kinase;
85 FDA – Food and Drug Administration; GFP – Green fluorescent protein; GM-CSF - Granulocyte-
86 macrophage colony-stimulating factor; HEK – human embryonic kidney; IFN – Interferon; IL –
87 Interleukin; IVIG - intravenous immunoglobulins; LPS – Lipopolysaccharide; MAMP - microbe-
88 associated molecular patterns; LukAB – Leukocidin AB; MWS – Muckle-Wells syndrome; NLR – Nod-
89 like receptor; NLRP3 – NACHT, LRR and PYD domains-containing protein 3; PBMC - peripheral blood
90 monocytic cells; PIP_3 - phosphatidylinositol (3,4,5)-trisphosphate; PMA - Phorbol-12-myristate-13-
91 acetate; PVL - Panton Valentine Leukocidin; SH - Src homology; TH - Tec homology; TLR – Toll-like
92 receptor; TNF – Tumor necrosis factor; XLA - X-linked agammaglobulinemia.

ACCEPTED MANUSCRIPT

ACCEPTED MANUSCRIPT

93 **INTRODUCTION**

94 The human immune system relies on both innate and adaptive mechanisms to defend the host
95 against infections, e.g. from pathogenic bacteria such as *Staphylococcus aureus*. Initial pathogen
96 sensing by the innate immune system employs so-called pattern recognition receptors (PRR), e.g.
97 Toll-like receptors (TLR) and Nod-like receptors (NLRs). Their activation by microbe-associated
98 molecular patterns (MAMPs) or invader-induced cellular insults leads to the production of pro-
99 inflammatory cytokines which establish an inflammatory state and are critical in activating adaptive
100 immunity [1]. Conversely to other cytokines, the important pro-inflammatory cytokine Interleukin (IL)-
101 1β is induced ('primed') at the mRNA level, but requires processing and secretion initiated by NLR
102 activation [2]. NLRP3, the most prominent NLR member, is activated by various pathogenic,
103 environmental and endogenous stress-related insults and thus plays a role in microbe-elicited as well
104 as sterile inflammation [3, 4]. Upon activation, NLRP3 assembles a so-called 'inflammasome' complex
105 with the adaptor ASC and caspase-1 leading to caspase auto-activation and consequent proteolytic
106 cleavage of pro-IL-1β into bioactive IL-1β for subsequent secretion [2]. The latter is a vital step in host
107 defense against infectious agents such as *S. aureus* [5]. Interestingly, the IL-1 axis also has
108 pathophysiological significance, as exemplified by autoinflammatory periodic fever syndromes, such
109 as Muckle-Wells syndrome (MWS), in which rare gain-of-function polymorphisms in NLRP3 lead to
110 spontaneous inflammasome activation [4, 6]. Furthermore, NLRP3 inflammasome activity has been
111 implicated in a diverse range of complex human diseases including gout, rheumatoid arthritis, type 2
112 diabetes, atherosclerosis and neurodegeneration [4]. The NLRP3 inflammasome can thus be
113 considered an attractive therapeutic target but efforts to develop inflammasome inhibitors have
114 been hampered by an incomplete knowledge regarding the identity and role of the molecular steps
115 involved in activating and regulating the inflammasome. Additionally, how the so far proposed
116 experimental inhibitors work is unclear. Thus the identification of well-defined and therapeutically
117 tractable regulatory proteins would be highly desirable.

ACCEPTED MANUSCRIPT

118 Bruton's Tyrosine Kinase (BTK) has long been regarded as a protagonist in adaptive antimicrobial
119 defense, since in the 1990s *BTK* mutations were discovered to be the cause for X-linked
120 agammaglobulinemia (XLA) [7], the first described primary immunodeficiency [8]. XLA, also termed
121 Bruton's disease, is characterized by the almost complete absence of B cells and, consequently,
122 antibodies, leading to severe immunodeficiency. More recently, BTK has also become appreciated as
123 an important therapeutic target, for example in B cell malignancies which are characterized by
124 continuous B cell receptor signaling *via* BTK [9]. Promising results have been obtained using FDA-
125 approved ibrutinib (PCI-32765), an orally-administered, selective and covalent BTK inhibitor, in
126 mantle cell lymphoma and chronic lymphocytic leukemia trials. Ibrutinib was both efficacious and
127 well-tolerated [10, 11]. *BTK* encodes a cytoplasmic protein tyrosine kinase expressed highly in B cells – in
128 the latter from very early stages of development controlling development, survival, differentiation
129 and activity [12, 13]. Additionally, *BTK* is also expressed in cells of the myeloid lineage, including
130 macrophages, neutrophils, mast cells, and dendritic cells [1,2], so that a contribution of the myeloid
131 compartment to the overall phenotype of XLA cannot be excluded. BTK contains several functional
132 domains (Fig. 1A): an N-terminal pleckstrin homology (PH) domain that binds phosphatidylinositol
133 (3,4,5)-trisphosphate (PIP_3), towards which BTK can translocate from the cytoplasm to PIP_3-
134 containing membranes; this property is abrogated in *Xid* (X-linked immunodeficiency) mutant mice
135 (R28C mutation) which exhibits, like Btk-deficient (*Btk*$^{-/-}$) mice, characteristics similar to the human
136 XLA phenotype, albeit the phenotype is less severe [14]. BTK furthermore features central Tec
137 homology (TH), Src homology (SH) 3 and SH2 domains involved in protein-protein interactions, and a
138 C-terminal catalytically active kinase domain. Two critical tyrosine phosphorylation sites, Y223 and
139 Y551, play a pivotal role in the activation of BTK. Y551 is first trans-phosphorylated by upstream Syk
140 or Lyn kinases which promotes the catalytic activity of BTK, with subsequent auto-phosphorylation at
141 position Y223. A known downstream target of BTK is phospholipase C but additional signaling
142 pathways regulating cell proliferation, differentiation and apoptosis have been shown to at least
143 partially depend on BTK function [12, 15]. Since XLA can be adequately managed clinically by regular
144 administration of intravenous immunoglobulins (IVIG) and antimicrobial therapy [14], a BTK-related

ACCEPTED MANUSCRIPT

145 defect in the humoral arm of the adaptive immune system has been taken as the primary
146 immunological explanation for the observed severe susceptibility of XLA patients for pyogenic
147 bacteria such including *S. aureus.* However, it is known that immunity against these bacteria also
148 strongly depends on innate immunity exerted by macrophages and neutrophils [16, 17], posing the
149 question whether XLA might also encompass BTK-related defects in the innate immune system.

150 We show here that BTK is a critical NLRP3 inflammasome regulator in both humans and mice and
151 thus functions in a key innate immune process. Inflammasome activity was found impaired in *Btk*-
152 deficient mice and XLA patients, suggesting that the XLA phenotype may indeed encompass the first
153 known primary genetic inflammasome deficiency. Furthermore, we demonstrate that
154 pharmacological BTK inhibition is able to block IL-1β release in a murine *in vivo* model as well as
155 human primary cells from healthy donors, MWS and Ibrutinib-treated patients.

ACCEPTED MANUSCRIPT

ACCEPTED MANUSCRIPT

156 **METHODS**

157 **Reagents.** Nigericin, Lipopolysaccharide (LPS), Phorbol-12-myristate-13-acetate (PMA) and
158 Ionomycin were purchased from Invivogen, ATP from Sigma, ibrutinib and CGI1746 from
159 Selleckchem, recombinant Granulocyte-macrophage colony-stimulating factor (GM-CSF) or M-CSF
160 from Prepro-Tech, Ficoll from Merck Millipore. Antibodies are listed in Supplemental Information.

161 **Study subjects and sample acquisition.** All human subjects provided written informed consent in
162 accordance with the Declaration of Helsinki and the study was approved by the local ethics
163 committees. Detailed information regarding buffy coats and blood samples from healthy donors,
164 XLA, MWS and ibrutinib-treated patients is provided in Supplemental Information.

165 **Isolation and stimulation of primary immune cells.** Peripheral blood mononuclear cells (PBMCs)
166 from healthy donors and XLA patients were isolated from whole blood using Ficoll density gradient
167 purification, primed with 10 ng/ml LPS for 3 h, and stimulated with 15 µM Nigericin for 1 h, or
168 instead with 50 ng/ml PMA and 1 µM Ionomycin for 4 h. PBMC from MWS were treated with 10
169 ng/ml LPS, 1 mM ATP concomitantly with 60 µM ibrutinib or a DMSO control for 4 h. For macrophage
170 differentiation, monocytes were purified by positive selection from PBMC (from buffy coats using
171 Ficoll purification) using anti-CD14 magnetic beads (Miltenyi Biotec, >90% purity), differentiated into
172 macrophages (GM-CSF for 5 days). The resulting Monocyte-derived macrophages (MoMacs) were
173 primed with 300 ng/ml LPS for 3 h and pre-treated with ibrutinib at 20 µM or 60 µM for 10 min
174 before stimulation with 15 µM Nigericin or the indicated amounts of LukAB or Panton Valentine
175 Leukocidin (PVL) for 1 h. Further details provided in Supplemental Information.

176 **Plasmid constructs.** ASC, NLRP3 and BTK coding sequences in pENTR clones were generated as
177 described in [18] and Supplemental Information.

178 **Cell culture.** All cells were cultured at 37 °C and 5% CO_2 in DMEM or RPMI supplemented with 10%
179 fetal calf serum, L-glutamine (2 mM), penicillin (100 U/ml), streptomycin (100 µg/ml) (all from Life
180 Technologies) unless described otherwise in Supplemental Information. THP-1 'Null' cells (Invivogen)

ACCEPTED MANUSCRIPT

181 stably express a non-targeting shRNA and were referred to throughout as 'THP-1' cells unless
182 otherwise stated. NLRP3-deficient THP-1 cells express an NLRP3-targeting shRNA (Invivogen). iGluc
183 THP-1[19] and THP-1 cells with stable BTK knockdown and corresponding mock cells [20] were kind gifts
184 of V. Hornung, Institute of Molecular Medicine, Munich, and R. Morita, Keio University School of
185 Medicine, Tokyo, respectively. ASC-mCerulean expressing immortalized macrophages or THP-1 cells
186 were described previously [21, 22].

187 **Mice and generation of BMDM.** Bone marrow (BM) cells were isolated from femurs and tibiae of 8-
188 12 week old *Btk* KO [23] mice and wild type littermates (all C57BL/6 background), grown and
189 differentiated using GM-CSF (M1 polarization) or M-CSF (M2 polarization). Cells were always counted
190 and re-seeded prior to *in vitro* assays to ensure equal cell numbers. For *in vivo* infections, 8 week old
191 C57BL/6 female mice (Jackson Laboratories) were used. All mouse colonies were maintained in
192 specific-pathogen free conditions. All animal experiments were approved by local authorities and
193 done in accordance with local institutional guidelines and animal protection laws as detailed in
194 Supplemental Information.

195 **Mass spectrometry analysis.** THP-1 'Null' cells (Invivogen) labelled to 97% with "light", "medium-
196 heavy" and "heavy" SILAC medium were primed with 300 ng/ml PMA for three hours and left to rest
197 overnight. The next day the cells were detached and either left unstimulated (light) or stimulated
198 with 15 µM Nigericin for 5 minutes (medium) or 10 minutes (heavy). After washing with ice-cold PBS
199 (containing phosphatase and protease inhibitors, Roche), cells pellets were snap-frozen and stored at
200 -80 °C prior to analysis. Further details on phosphopeptide enrichment, LC-MS/MS, peptide
201 identification are described in Supplemental Information.

202 **ELISA.** IL-1ß, IL-2, Tumor necrosis factor (TNF), interferon (IFN) γ in supernatants were determined
203 using half-area plates by ELISA (Biolegend) using triplicate points on a standard plate reader.

204 **RT qPCR.** mRNA was isolated using the RNeasy Mini Kit on a Qiacube robot (both Qiagen) transcribed
205 to cDNA (High Capacity RNA-to-cDNA Kit; Life Technologies) and *Il1b, Nlrp3, IL1B and NLRP3* mRNA
206 expression quantified in triplicates relative to TBP using TaqMan primers (Life Technologies) on a

ACCEPTED MANUSCRIPT

207 real-time cycler (Applied Biosystems; 7500 fast) as described in [18]. Comparable CT values for TBP (not
208 shown) in all treatment groups confirmed equal cell numbers.

209 **ASC speck formation assay and confocal microscopy.** $4x10^4$ Human embryonic kidney (HEK) 293T
210 cells were plated, transiently transfected, fixed with 100% methanol, stained for nucleic acids (To-
211 pro-3, Thermo Fisher) and BTK-HA (anti-HA-Alexa 594). Immortalized *Nlrp3* KO macrophages
212 overexpressing NLRP3-FLAG and ASC-mCerulean were pretreated with ibrutinib or CGI1745 (and a
213 solvent control) for 10 min or 60 min, respectively, before stimulation with either 5 µM Nigericin (Life
214 Technologies) for 60 min or 1 mM Leu-Leu-OMe•HCl (Chem-Impex) for 90 min, then fixed (4%
215 formaldehyde), and nucleic acids stained (DRAQ5, eBioscience). Details regarding analysis using a
216 Zeiss confocal microscope and image quantification using ImageJ or CellProfiler are described in
217 Supplemental Information.

218 **Pro-IL-1β and caspase-1 cleavage.** Equal amounts of cells were primed and then stimulated in Opti-
219 MEM media (Gibco). Proteins in supernatants was precipitated by methanol (VWR International) and
220 chloroform (Sigma). Cells were lysed in a RIPA buffer with protease inhibitors (Sigma). Where
221 applicable, recombinant Protein A was added prior to precipitation to control for equal precipitation.
222 15% and 12% SDS-PAGE gels were used for protein from supernatants and whole cell lysates,
223 respectively, and probed with the indicated antibodies.

224 **Co-immunoprecipitation.** HEK293T were transfected using $CaPO_4$ and lysed 48 hours later in a buffer
225 (50 mM Tris pH 8, 280 mM NaCl, 0.5% NP-40, 0.2 mM EDTA, 2 mM EGTA, 10% glycerol, 1 mM DTT)
226 with protease/phosphatase inhibitors (Roche). Cleared lysates were subjected to
227 immunoprecipitation of the BTK-Protein A fusion protein with Dynabeads (M-280 Sheep Anti-Mouse
228 IgG, Thermo Fisher Scientific). Washed beads were boiled in loading buffer and applied to SDS-PAGE
229 and immunoblot, see Supplemental Information.

230 **Crosslinking of ASC-oligomers.** $2x10^6$ THP-1 ASC-mCerulean cells were primed with 300 ng/ml LPS for
231 2 hours, then treated with 60 µM ibrutinib for 1 hour and then with 15 µM Nigericin for 1 hour. After

ACCEPTED MANUSCRIPT

232 washing with PBS, cells were lysed and lysates and pellets cross-linked using DSS and analyzed as
233 described in [24] and Supplemental Information.

234 **Flow cytometry and phospho-flow.** Whole blood from healthy donors and XLA patients was
235 subjected to standard cell surface staining and flow cytometry using anti-CD3-FITC, -CD19-Pacific
236 Blue, -CD14-PE and -CD11b-APC using a standardized protocol and identical flow cytometer settings
237 for all donors. For phosflow analysis, the indicated primed cells were treated and then fixed (Lyse/Fix
238 Buffer, BD), permeabilized with 1 ml of cold methanol, Fc-receptors were blocked (Human AB serum)
239 and cells were stained with anti-Btk (pY551) PE, anti-Btk (pY223) BV421, and anti-total BTK Alexa
240 Fluor 647 Abs (all from BD). Corresponding isotype controls were from Immunotools. For further
241 details see Supplemental Information.

242 ***S. aureus* strains.** The community-acquired methicillin-resistant *S. aureus* strain USA300
243 bioluminescent derivative, LAC::*Lux:*, were grown according to standard microbiological practice and
244 used as indicated, see details in Supplemental Information.

245 ***In vivo* infection model.** Ibrutinib (6 mg/kg) in 3% DMSO and 5% corn oil in PBS or vehicle control was
246 injected i.v. via the retro-orbital vein in anesthetized mice on days -1, 0, 1, and topically on day 2 (6
247 mg/kg ibrutinib in 10 µL DMSO or vehicle control). On day 0 the dorsal backs of anesthetized mice
248 (2% isoflurane) were shaved, injected intradermally with $3x10^7$ CFU of *S. aureus* LAC::*Lux:* digitally
249 imaged on 1, 3, 7, 10 and 14, and total lesion size (cm^2) analyzed using ImageJ with a millimeter ruler
250 as a reference.

251 ***In vivo S. aureus* bioluminescent imaging.** Mice were anesthetized (2% isoflurane) and *in vivo*
252 bioluminescent imaging was performed (Lumina III IVIS, PerkinElmer) and total flux (photons/s)
253 within a circular region of interest measuring $1x10^3$ pixels was measured using Living Image software
254 (PerkinElmer) (limit of detection: $2x10^4$ photons/s).

255 **Purification of LukAB and PVL.** The pQE30 vector (Qiagen) was used to produce recombinant His-
256 tagged LukS-PV, LukF-PV, LukA and LukB as described in Supplemental Information using Ni-NTA

ACCEPTED MANUSCRIPT

257 affinity chromatography. Protein stock solutions were dialyzed against PBS/50 % glycerol, checked
258 for endotoxin contamination (<0.25 EU/ml; Lonza) and stored at -20°C until use. Single components
259 were mixed in equal molar ratio (IL-1β secretion was not detectable in stimulations using the single
260 components, not shown).

261 **Data analysis and statistics.** Data were analyzed in GraphPad Prism v.5.0 using Student's *t*-tests and
262 non-parametric Mann-Whitney-U or Wilcoxon matched-pairs signed rank tests as indicated. All tests
263 were two-tailed unless stated otherwise. A *P* value of <0.05 was generally considered statistically
264 significant and, even if considerably lower, marked as * throughout.

ACCEPTED MANUSCRIPT

ACCEPTED MANUSCRIPT

265 **RESULTS**

266 **BTK is rapidly phosphorylated upon NLRP3 inflammasome activation**

267 To identify novel NLRP3 regulators of the NLRP3 inflammasome we used unbiased triple SILAC
268 phospho-proteomics [25] in primed THP-1 macrophages activated by the microbial potassium
269 ionophore and NLRP3 agonist, Nigericin (see Methods). Differences in the phospho-proteome of
270 unstimulated cells vs. cells stimulated for 5 or 10 min - in order to capture early, NLRP3-proximal
271 events – included a phospho-peptide harboring the well-known BTK regulatory site, tyrosine 551
272 (Y551, Fig. 1A), which was significantly up-regulated 2.6-fold within 5 min of stimulation. Phospho-
273 flow cytometry analysis in primed THP-1 cells (Fig. 1B) and primary human monocyte-derived
274 macrophages (MoMacs, Fig. 1C) confirmed that whereas Y223 showed only subtle phosphorylation,
275 Y551 was rapidly and robustly phosphorylated, peaking at 5 min after Nigericin addition, indicating a
276 rapid activation of BTK by an NLRP3 inflammasome trigger.

277 **Pharmacological inhibition of BTK impairs inflammasome activation**

278 To assess if such BTK activation translated to an effect on inflammasome function we investigated
279 NLRP3-dependent IL-1β release. THP-1 cells pre-treated with the FDA-approved inhibitor, ibrutinib
280 (PCI-32765), indeed responded with reduced IL-1β release (Fig. 2A), despite comparable pro-IL-1β
281 and NLRP3 mRNA levels (Fig. 2B). This was confirmed in so-called iGluc THP-1 cells, in which IL-1β
282 release can be quantified in the form of a *Gaussia* luciferase assay (Fig. 2C) [19]. Importantly, in primary
283 MoMacs pharmacological BTK inhibition strongly decreased IL-1β (Fig. 2D) whereas the effect on TNF
284 release was minor (Fig. 2E). Similar results were obtained with an additional specific BTK inhibitor,
285 CGI1746 [26] (Fig. 2D,E). Generally, ibrutinib and CGI1746 did not show cytotoxicity at the
286 concentrations used here as assessed by simultaneous CCK8 viability testing (not shown). Minor
287 effects of BTK inhibition at the level of pro-IL-1β or NLRP3 mRNA (Fig. 2B) or secreted TNF (Fig. E)
288 suggest that the observed effect related directly to IL-1β processing rather than priming. Indeed pro-
289 IL-1β and caspase-1 processing in primary MoMacs were strongly reduced by both ibrutinib and

ACCEPTED MANUSCRIPT

290 CGI1746 (Fig. 2F). Collectively, this pharmacological approach implicated BTK in NLRP3
291 inflammasome function.

292 **Genetic ablation of BTK confirms a role in inflammasome activation**

293 To rule out off-target effects and further confirm a role of BTK in NLRP3 inflammasome function, we
294 employed genetic ablation of BTK and first analyzed IL-1β release from bone-marrow derived
295 macrophages (BMDMs) from *Btk* knock-out (KO) mice. Evidently, IL-1β release (Fig. 3A), but not *Il1b*
296 or *Nlrp3* mRNA synthesis (Fig. 3B), was strongly reduced in both GM-CSF- and M-CSF-differentiated
297 *Btk* KO vs. WT BMDMs. THP-1 cells in which BTK was constitutively downregulated by shRNA showed
298 a reduced IL-1 release compared to the corresponding mock THP-1 cells in response to NLRP3-
299 dependent inflammasome stimuli Nigericin, monosodium urate (MSU) and ATP but not the AIM2
300 inflammasome stimulus poly(dA:dT) (Fig. 3C). More importantly, we were able to compare PBMC
301 from healthy donors and matched XLA patients with genetically and cytometrically confirmed BTK
302 deficiency (see Supplemental Information and Fig. S1). PMA+Ionomycin, a non-NLRP3-dependent [27]
303 and poorly IL-1β inducing stimulus, prompted IL-2 and IFNγ release from T cells, in which BTK is not
304 expressed and thus is functionally irrelevant [28] (Fig. 3D), thus indicating similar overall cellular
305 viability in PBMC preparations from healthy and XLA donors. However, IL-1β release in response to
306 NLRP3 activation by Nigericin, was substantially lower from XLA PBMC compared to healthy donors
307 (Fig. 3E), irrespective of whether priming was conducted with R848, or ATP used as an alternative
308 NLRP3 trigger (Fig. 3E). Although differences in IL-1β levels in response to ATP were not statistically
309 significant due to donor-to-donor variation, a clear trend towards lower IL-1β was clearly discernible.
310 As expected, secreted mature caspase-1 and IL-1β was also reduced in XLA PBMC compared to PBMC
311 from healthy donors (Fig. 3F), even though LPS-primed *IL1B* and *NLRP3* mRNA levels at the time of
312 NLRP3 agonist addition were higher (Fig. 3G). Thus, genetic ablation of BTK activity in both mice and
313 humans impairs NLRP3 inflammasome activity and confirms a role for BTK in the NLRP3
314 inflammasome.

ACCEPTED MANUSCRIPT

315 **BTK interacts directly with ASC and NLRP3 and promotes inflammasome formation**

316 Given the early phosphorylation of BTK and its effect on downstream caspase-1 cleavage, we
317 speculated whether BTK might directly interact with the core inflammasome components ASC and
318 NLRP3. Indeed, when expressed in HEK293T cells, BTK interacted with both ASC (Fig. 4A) and NLRP3
319 (Fig. 4B) in co-immunoprecipitations. Additionally, overexpression-induced ASC speck formation, a
320 surrogate visual readout for inflammasome formation [22], in HEK293T cells transfected with ASC- GFP
321 was significantly enhanced by BTK co-expression (Fig. 4C, quantified in Fig. 4D). Interestingly, a
322 spheroid ASC signal typical for ASC specks was surrounded by a spherical localization of BTK (Fig.
323 S2A). In agreement with earlier experiments, ibrutinib (Fig. 4E,F) and CGI1746 (Fig. S2B) reduced ASC
324 speck formation in stably ASC-mCerulean expressing murine macrophages [22] when treated with
325 Nigericin or the NLRP3 trigger, Leu-Leu-OMe, a lysosomal destabilizing agent [29]. Furthermore, the
326 potential for ASC cross-linking/oligomerization [24] in THP-1 cells stably expressing ASC-mCerulean was
327 enhanced by Nigericin stimulation but sensitive to ibrutinib (Fig. 4G). Collectively, BTK appears to
328 thus directly influence inflammasome activation at the level of NLRP3 and ASC.

329 **BTK functionality is required for full *S. aureus* toxin-elicited inflammasome activity**

330 BTK-deficient XLA patients suffer from recurrent bacterial infection with pathogens including *S.*
331 *aureus.* Based on the observation that Nigericin- and ATP-triggered IL-1β processing and secretion
332 were impaired in XLA patients (*cf.* Fig. 3), we wondered whether IL-1β release induced by the *S.*
333 *aureus* toxins, PVL and LukAB – which both activate NLRP3 (see [30, 31] and Figs. 5A, S3) – also required
334 BTK. Indeed, BTK inhibition (Fig. 5B) and stable shRNA-mediated BTK knock-down (Fig. 5C) in THP-1
335 cells and ibrutinib-treatment in primary MoMacs (Fig. 5D) strongly reduced IL-1β release in response
336 to PVL and LukAB. Additionally, in LPS-primed XLA PBMC, LukAB led to reduced IL-1β cleavage
337 compared to healthy donors (Fig. 5E). Since LPS does not occur in Gram-positive bacteria and *S.*
338 *aureus* instead activates TLR2 [32], the TLR2 agonist Pam_3CSK_4 was also used for priming instead of LPS.
339 Again, TLR2-primed PBMC from XLA patients showed reduced cleaved IL-1β compared to healthy

ACCEPTED MANUSCRIPT

340 donors in response to LukAB (Fig. 5E). These genetic and pharmacological *in vitro* results suggest that
341 *in vivo* BTK might play a role in NLRP3 inflammasome/IL-1β-dependent host defense, as well as
342 pathophysiological auto-inflammation.

343 **BTK inhibition negatively affects IL-1β-dependent *S. aureus* clearance *in vivo* and blocks IL-1β**
344 **release in Muckle-Wells-Syndrome and ibrutinib-treated cancer patients *ex vivo*.**

345 We next explored the possibility whether BTK inhibition would affect the outcome of IL-1β-
346 dependent infection in an *in vivo* setting. Murine experimental models of *S. aureus* skin infection
347 dependent on Nlrp3/ASC-inflammasome-dependent IL-1β for clearance [5, 33]. We therefore applied
348 ibrutinib treatment to C57BL/6 mice intradermally infected with a bioluminescent community-
349 acquired MRSA strain (USA300 LAC::*lux*) [33]. Ibrutinib-treated mice showed increased bacterial burden
350 as measured by *in vivo* bioluminescent signals (Fig. 6A, B) compared with vehicle-treated control
351 mice. They also developed larger skin lesions (Fig. 6C and Fig. S4). Although additional *in vivo* effects
352 of ibrutinib cannot be ruled out, our data suggest a relevance for BTK in inflammasome-related host
353 defense *in vivo*.

354 Our results so far posed the question whether BTK may rather be a plausible point of therapeutic
355 intervention to target the many human inflammasome/IL-1β-related inflammatory processes or
356 disorders [4]. MWS is a autoinflammatory disease caused by gain-of-function mutations in the NLRP3
357 gene, *CIAS*, and is characterized by excessive IL-1β release compared to healthy donors (Fig. S6). To
358 explore if this phenotype could be ameliorated by BTK inhibition, we triggered IL-1β release by LPS
359 (no second stimulus required due to NLRP3 auto-activation, see [34]) in PBMC from four MWS patients
360 in the absence or presence of ibrutinib. As shown in Fig. 6D, LPS-dependent IL-1β and caspase-1
361 release was strongly reduced for all assessed patients, and the level of inhibition corresponded to the
362 dose of ibrutinib (Fig. 6E). General toxicity or anti-inflammatory effects were ruled out using cytokine
363 release and viability tests (not shown). Thus, pharmacological BTK inhibition blocked excessive IL-1β
364 release that characterizes the autoinflammatory MWS. To gain a first insight whether application of

ACCEPTED MANUSCRIPT

365 ibrutinib in human patients would affect inflammasome activity *in vivo*, we stimulated PBMC from
366 male cancer patients receiving ibrutinib daily *ex vivo* and compared their ability to process or release
367 IL-1β or caspase-1 in response to NLRP3 triggers Nigericin and/or ATP by immunoblot or ELISA,
368 respectively (Fig. 6G,F), whereas TNF release was comparable (Fig. 6H). Evidently, *in vivo* application
369 of ibrutinib specifically correlated with reduced *ex vivo* IL-1β and caspase-1 processing and lower IL-
370 1β release in these patients compared to individuals not receiving ibrutinib. Collectively, our data
371 therefore suggest that BTK inhibitors may block the NLRP3 inflammasome *in vivo* in patients.

ACCEPTED MANUSCRIPT

ACCEPTED MANUSCRIPT

372 **DISCUSSION**

373 In the present work we show that Bruton's Tyrosine Kinase is a critical regulator of NLRP3
374 inflammasome activation in both humans and mice. This is illustrated by significant NLRP3
375 inflammasome loss-of-function phenotypes observed in functionally *BTK*-deficient cells, patients and
376 mice, and effects of pharmacological inhibition of BTK in an *in vivo S. aureus* infection model, which is
377 congruent with inefficient bacterial control evidenced in human XLA patients and *Xid* or *Nlrp3*$^{-/-}$ mice
378 [12, 33]. Additionally, our molecular analysis suggests that BTK regulates (and that consequently BTK
379 inhibitors might act on) the inflammasome proximally to NLRP3 and ASC, as evidenced by interaction
380 and co-localization of BTK with these inflammasome components. Furthermore we demonstrate that
381 in human primary macrophages (as well as their murine counterparts), BTK inhibition impaired IL-1β
382 processing and release. In blood samples from MWS patients BTK inhibition strongly reduced this
383 pathologically relevant inflammatory event. Notably, reduced IL-1β secretion was also observed in
384 PBMC from patients receiving ibrutinib *in vivo*. These findings represent considerable advances
385 regarding our understanding of the NLRP3 inflammasome, its therapeutic tractability as well as BTK-
386 related immunodeficiency, which warrant further discussion.

387 Firstly, our data significantly expand upon the so far known roles of BTK and highlight that BTK not
388 only critically contributes to adaptive immunity but is in fact also a key player in innate immunity.
389 Although few reports described a role for BTK in TLR [35, 36] and Fc receptor signaling [26], recruitment [37]
390 and development [13] in myeloid cells, the abovementioned insights were almost exclusively gained for
391 the murine system or human cell lines. Whether BTK played a prominent role in human innate
392 immunity thus remained somewhat unaddressed. It is also for the murine system that Ito et al.
393 recently provided a first glimpse into a possible role for BTK in inflammasome activation [20]. In this
394 study, BTK loss or inhibition in murine cells reduced IL-1β release. Our study in primary cells from
395 healthy volunteers, XLA, MWS and Ibrutinib-treated patients now provide evidence that BTK is
396 indeed a key regulator of the NLRP3 inflammasome in humans. How the observed residual amounts
397 of IL-1β released from XLA PBMC (Fig. 3D/E) that can be reduced further (Fig. 6F and S5) by an NLRP3

ACCEPTED MANUSCRIPT

398 inhibitor with unknown target, MCC950 [38], warrants further exploration. It seems plausible that the
399 *BTK* mutations identified in the patients studied here (see Supplemental information) display low
400 residual activity [39] or expression of BTK that is sufficient for low inflammasome activity but too low to
401 support the development of B cells and thus leading to clinical XLA; alternatively, BTK may only be
402 required for one of potentially several NLRP3 inflammasome pathways [40]. Nevertheless, our study
403 supports a notion that regards BTK as a master regulator of myeloid cell functions spanning the
404 entire functional spectrum from development, via initial pathogen recognition by TLR, to initiation of
405 inflammation via the NLRP3 inflammasome, to post-adaptive functions involving the response to
406 antibodies bound via Fc receptors. The versatility of BTK to participate in these diverse processes is
407 staggering and clearly warrants further exploration, not least to investigate cross-talk between the
408 different signaling pathways as well as closely define how pharmacological inhibition of BTK affects
409 these different BTK-dependent immune functions.

410 This is indeed necessary to explore potential therapeutic opportunities that could be deduced from
411 the observation that BTK inhibitors reduce NLRP3-dependent IL-1β release. Human macrophages,
412 which can be effectively blocked in their ability to release IL-1β as shown here, have been seen as
413 primary mediators in many inflammatory disorders. For example, in experimental mouse models for
414 atherosclerosis cholesterol crystals contribute to disease progression in a macrophage/IL-1
415 dependent way [41]. Similarly, in Alzheimer's models amyloid-β-triggered neuro-inflammation depends
416 on NLRP3 [42]. Targeting the IL-1 axis via BTK may have considerable advantages over previously
417 proposed strategies: for example, for proposed inhibitors like MCC950 [38], though highly effective, the
418 precise mechanism of action and the actual molecular target seem unclear at current. Biological-
419 based anti-IL-1 therapies, though proven and FDA-approved, target inflammasome-distal events.
420 Targeting the inflammasome via BTK might eventually overcome some of these disadvantages by
421 focusing on a well-studied and well-defined molecular target, BTK, and an NLRP3 inflammasome (and
422 thus caspase/IL-1β processing) proximal event. Use of ibrutinib in treating human patients suffering
423 from MWS (*cf.* Fig. 6), acute stroke – as hinted to by Ito et al. [20] – , or atherosclerosis now should be

ACCEPTED MANUSCRIPT

424 considered and is encouraged by the observed good tolerability and efficacy of BTK inhibitors in the
425 cancer setting [10, 11], primary human immune cells (*cf.* Figs. 2-6) and even human platelets, as
426 suggested by our most recent study [43]. The data shown in Fig. 6F,G suggest that BTK inhibition may
427 be considered for blocking inflammasome activity *in vivo*. Even if administration would have to be
428 temporary (e.g. to avoid adverse effects from infection, see below), a temporary blockade of the IL-1
429 axis may help break a vicious cycle of chronic inflammation.

430 For effective therapeutic exploitation additional details need, however, to be clarified. Firstly, as with
431 any pharmacological inhibitor, off-target effects, i.e. the possibility of other kinases apart from BTK
432 being affected by ibrutinib or other "BTK"-inhibitors, cannot be entirely ruled out and requires
433 further investigation. Secondly, although a direct interaction with NLRP3 and ASC has been
434 demonstrated by us (*cf.* Fig. 4), it remains to explored how exactly BTK participates in the
435 inflammasome activation process. Ito *et al.* rule out an effect of Ca^{2+} signaling and by measuring
436 additional cytokines or transcript levels we can rule out that BTK ablation primarily affects caspase-1
437 or IL-1β cleavage or release via TLR-dependent priming, although this would have been conceivable
438 due to the role of BTK in TLR signaling [35]. The SH2 and SH3 domains found in BTK are well-known
439 motifs for protein-protein interactions so that BTK may act as a scaffold protein for inflammasome
440 nucleation or extension. But since ibrutinib targets BTK kinase activity it seems unlikely that BTK only
441 acts as a molecular scaffold but rather participates as a kinase, possibly at the level of ASC
442 phosphorylation [20]. The verification of ASC as a BTK interactor and substrate should be the subject of
443 future studies. Another important question to be addressed is what links the exposure of cells to
444 upstream NLRP3 agonists with BTK activation. Studying the role of the PH domain, a common motif
445 for receptor/membrane engagement , or different reported gain- or loss-of-function mutants such as
446 the *Xid* loss-of-function mutation (R28C) in the assays described here may shed light on these
447 important mechanistic questions in the future.

448 BTK acting as a novel inflammasome component would make any genetic BTK insufficiency also a
449 genetically determined functional NLRP3 inflammasome deficiency. Our work thus supports the

ACCEPTED MANUSCRIPT

450 notion that BTK-mediated human XLA phenotype may represent the first reported genetic functional
451 NLRP3 inflammasome deficiency in humans. Given that *S. aureus* toxin-mediated release is BTK-
452 dependent (Fig. 5) and BTK-dependent IL-1β production is required for bacterial clearance in skin *S.*
453 *aureus* infection in mice[33] (Fig. 6A-C), human inflammasome-deficient patients would be expected to
454 show a susceptibility to pyogenic bacteria, e.g. *S. aureus*. This is indeed a clinical feature in XLA
455 patients [12, 14]. It can be speculated whether high dose IVIG and antibiotics therapy routinely applied
456 to XLA patients may mask a simultaneous NLRP3 inflammasome deficiency contributing to bacterial
457 susceptibility in XLA patients. Of note, a certain fraction of patients in ongoing clinical trials with
458 ibrutinib show moderate to severe infections with the same pathogens frequently encountered in
459 XLA patients despite unaltered antibody levels [10, 11], i.e. a remaining adaptive/humoral defense
460 component. Potentially, this temporary bacterial susceptibility conferred by BTK inhibition may be
461 significantly attributable to temporary inflammasome inhibition. Further studies should address this
462 possibility in ongoing clinical trials with ibrutinib and explore the notion of a potential inflammasome
463 deficiency to contribute to immunodeficiency in XLA patients.

464 Collectively, the data presented here imply that in humans and mice, unexpectedly, two protagonists
465 of innate and adaptive immunity, NLRP3 and BTK, cooperate in the activation of the inflammasome,
466 an innate defense mechanism that is critical for the activation of adaptive immunity. Our data in
467 human primary cells provide a rationale for further investigations on the molecular level and for
468 exploring therapeutic implications. Targeting the NLRP3 inflammasome at the level of BTK may bring
469 inflammasome targeting unexpectedly within reach if larger clinical studies confirm the observed
470 effects and FDA-approval was extended beyond B cell malignancies. The growing number of BTK
471 inhibitors developed for the treatment of hematological malignancies may thus be interesting for
472 clinicians working on the many reported IL-1β-driven inflammatory diseases to follow, in order to
473 glean insights into how to possibly apply BTK inhibition to their clinical settings.

ACCEPTED MANUSCRIPT

474 **FIGURE CAPTIONS**

475 **Figure 1: BTK is rapidly phosphorylated in myeloid cells upon NLRP3 inflammasome triggering.** (A)
476 Domains, phospho-sites (red) and the regulated phospho-peptide (grey) in BTK. PMA-primed THP-1
477 cells (B) or LPS-primed human primary MoMacs (C) were stimulated with Nigericin, stained and
478 analyzed by flow cytometry. ΔMFI differences for each antibody-isotype pair are given. One
479 representative of three experiments each is shown.

480 **Figure 2: Ablation of BTK impairs NLRP3-inflammasome activity.** (A) IL-1β release from PMA-
481 differentiated and Nigericin-treated THP-1 cells pre-incubated with ibrutinib (60 µM) (B) mRNA levels
482 before Nigericin addition. (C) IL-1β-*Gaussia* levels assessed as in [19]. Cleaved IL-1β (D,F), caspase-1 (F)
483 and TNF (E) from primed and Nigericin-treated human primary MoMacs pre-treated with DMSO
484 (mock), ibrutinib or CGI-1746 for 10 min. In (A) one out of two, in (B) one out of three, in (C) one out
485 of two experiments, and in (D and E) two out of five and in (F) one out of three donors are shown.
486 Means +SD are shown and two-sided Student's *t*-tests were used. Comparison to the DMSO control
487 (grey bar). *=p<0.05.

488 **Figure 3: Genetic ablation of BTK in primary immune cells impairs NLRP3-mediated IL-1β release.**
489 (A) IL-1β release from equal numbers of GM-CSF or M-CSF-differentiated, LPS-primed and Nigericin-
490 treated WT or *Btk* KO BMDMs (mean+SEM). (B). RT-qPCR (mean+SEM) prior to Nigericin addition (B).
491 (C) IL-1β release from primed THP-1 cells expressing either a non-targeting (Mock) or BTK-shRNA.
492 (D,E) IL-1β, IL-2 and IFNγ release from LPS-primed PBMC from male XLA patients and age-matched
493 male healthy donors (mean ±SEM of biological replicates, each symbol represents one donor).
494 Supernatnat immunoblot (F), or RT-qPCR relative to *TBP* (mean+SD) (G) of the stimulated PBMC.
495 Pooled data from 3 mice (biological replicates)/group (one out of two identical experiments) in (A
496 and B), and from six vs. three donors (biological replicates; mean+SEM in grey) in (D and E) are
497 shown, respectively. In (C) one representative of two experiments, in (F,G) two vs. four donors are
498 shown, respectively. In (A)-(C) and (G,H) a Student's *t*-test, in (D and E) a Mann-Whitney-U test was
499 used. *=p<0.05.

ACCEPTED MANUSCRIPT

500 **Figure 4: BTK directly interacts with ASC and NLRP3 and promotes inflammasome formation.** (A, B)
501 Immunoblot of transfected HEK293T cells. * = non-specific loading control. (C) Confocal microscopy
502 of fixed and stained transfected HEK293T cells (Scale bar = 200 µm), and (D) quantification thereof
503 (E, F) Representative fluorescence microscopy images of ASC specks (E) and quantification thereof (F)
504 from immortalized *Nlrp3* KO macrophages overexpressing NLRP3-FLAG ASC-mCerulean. Scale bar 20
505 µm. (G) DSS cross-linking of ASC from primed and Nigericin-treated THP-1-ASC-mCerulean cells. In
506 (A)-(D) one out of two, in (E) and (G) one out of three identical experiments is shown. (F) shows the
507 combined analysis of three experiments. In (D) and (F) a Student's *t*-test was used. *=p<0.05.

508 **Figure 5: BTK functionality is required for full *S. aureus* toxin-elicited inflammasome activity.** (A) IL-
509 1β release from PMA-differentiated 'Null' (control, A and B) or NLRP3-deficient (B) THP-1 inhibitor
510 pre-treated (B only) and stimulated as indicated. DB = LukAB dialysis buffer. (C) Primed THP-1 cells
511 expressing either a non-targeting (Mock) or BTK-shRNA were stimulated as indicated. (D) Primed
512 human primary MoMacs analyzed as in Fig. 2E/F but treated with LukAB or PVL. (E) Supernatant
513 immunoblot of LPS or Pam_3CSK_4-primed PBMC from male XLA patients and age-matched male
514 healthy donors. In (A)-(C) one out of two, in (D) and (E) two out of two identical experiments are
515 shown. In all graphs means +SD are shown and a Student's *t*-test was used. *=p<0.05.

516 **Figure 6: BTK inhibition negatively affects IL-1β-dependent *S. aureus* clearance *in vivo* and blocks**
517 **excessive IL-1β release in Muckle-Wells-Syndrome patients *ex vivo*.** Mean total flux (photons/s) ±
518 SEM (A) and mean total lesion size (cm^2) ± SEM (C) from C57BL/6 mice (n=10 per group) treated with
519 vehicle or ibrutinib and inoculated intradermally with bioluminescent MRSA USA300 LAC::*lux*. (B)
520 representative *in vivo* bioluminescent signals. (D) LPS-induced IL-1β or caspase-1 release from LPS-
521 stimulated[34] MWS patient PBMC. In (E) ibrutinib was titrated from 60, to 30, to 15, to 7.5 µM for two
522 MWS patients, one patient is shown (mean +SD). (F-H) IL-1β, caspase-1, TNF and/or IL-6 cleavage
523 and/or release (mean ±SEM of biological replicates, each symbol represents one donor) from PBMC
524 from male cancer patients daily receiving ibrutinib and male healthy donors. P=blotting control.
525 Pooled data from four vs. three donors shown in (F) and from eight vs. two donors in (G) or three vs.

ACCEPTED MANUSCRIPT

526 four donors in (H) (means ±SEM of biological replicates, each symbol represents one donor). In (A),
527 (C), (G) and (H) a Mann-Whitney-U test, in (D) a Wilcoxon matched-pairs signed rank test, and in (E) a
528 Student's *t*-test was used. *=p<0.05.

529 **Author contributions**

530 XL, TP, OOW, TMD, MDG, AS, CP, SD, ED, LM, SW, MFW and CB performed experiments; XL, TP,
531 OOW, TMD, MDG, AS, CP, SD, ED, LM, MFW, BM, BS, CW and ANRW analyzed data; XL, HK, NR, JKD,
532 MR, JS, DH, SS, BG and CB were involved in patient recruitment and sample acquisition; ANRW wrote
533 the manuscript and XL, TP, OOW, TMD, AS, AY, ED, SV, DH, BG, CB and CW provided valuable
534 comments. All authors approved the final manuscript. ANRW coordinated the study.

535 **Acknowledgements**

536 We gratefully acknowledge T. Proikas-Cezanne and D. Bakula for assistance with confocal
537 microscopy, I. Droste-Borel for help with mass spectrometry sample preparation, and M. Löffler and
538 I. Schäfer for help with supplying healthy donor and MWS patient samples, respectively. We thank all
539 study subjects and their families for participating in the study.

ACCEPTED MANUSCRIPT

ACCEPTED MANUSCRIPT

540 **References**

541 1. Kawai T, Akira S. Toll-like receptors and their crosstalk with other innate receptors in
542 infection and immunity. Immunity 2011; 34:637-50.
543 2. McGettrick AF, O'Neill LA. NLRP3 and IL-1beta in macrophages as critical regulators of
544 metabolic diseases. Diabetes Obes Metab 2013; 15 Suppl 3:19-25.
545 3. Chen GY, Nunez G. Sterile inflammation: sensing and reacting to damage. Nat Rev Immunol
546 2010; 10:826-37.
547 4. Broderick L, De Nardo D, Franklin BS, Hoffman HM, Latz E. The inflammasomes and
548 autoinflammatory syndromes. Annu Rev Pathol 2015; 10:395-424.
549 5. Miller LS, Pietras EM, Uricchio LH, Hirano K, Rao S, Lin H, et al. Inflammasome-mediated
550 production of IL-1beta is required for neutrophil recruitment against Staphylococcus aureus
551 in vivo. J Immunol 2007; 179:6933-42.
552 6. Hoffman HM, Mueller JL, Broide DH, Wanderer AA, Kolodner RD. Mutation of a new gene
553 encoding a putative pyrin-like protein causes familial cold autoinflammatory syndrome and
554 Muckle-Wells syndrome. Nature Genetics 2001; 29:301-5.
555 7. Tsukada S, Saffran DC, Rawlings DJ, Parolini O, Allen RC, Klisak I, et al. Deficient expression of
556 a B cell cytoplasmic tyrosine kinase in human X-linked agammaglobulinemia. Cell 1993;
557 72:279-90.
558 8. Bruton OC. Agammaglobulinemia. Pediatrics 1952; 9:722-8.
559 9. Hendriks RW. Drug discovery: New Btk inhibitor holds promise. Nat Chem Biol 2011; 7:4-5.
560 10. Burger JA, Keating MJ, Wierda WG, Hartmann E, Hoellenriegel J, Rosin NY, et al. Safety and
561 activity of ibrutinib plus rituximab for patients with high-risk chronic lymphocytic leukaemia:
562 a single-arm, phase 2 study. Lancet Oncol 2014; 15:1090-9.
563 11. Byrd JC, Furman RR, Coutre SE, Flinn IW, Burger JA, Blum KA, et al. Targeting BTK with
564 ibrutinib in relapsed chronic lymphocytic leukemia. N Engl J Med 2013; 369:32-42.
565 12. Khan WN. Colonel Bruton's kinase defined the molecular basis of X-linked
566 agammaglobulinemia, the first primary immunodeficiency. J Immunol 2012; 188:2933-5.
567 13. Fiedler K, Sindrilaru A, Terszowski G, Kokai E, Feyerabend TB, Bullinger L, et al. Neutrophil
568 development and function critically depend on Bruton tyrosine kinase in a mouse model of X-
569 linked agammaglobulinemia. Blood 2011; 117:1329-39.
570 14. Hendriks RW, Bredius RG, Pike-Overzet K, Staal FJ. Biology and novel treatment options for
571 XLA, the most common monogenetic immunodeficiency in man. Expert Opin Ther Targets
572 2011; 15:1003-21.
573 15. Qiu Y, Kung HJ. Signaling network of the Btk family kinases. Oncogene 2000; 19:5651-61.
574 16. Peschel A, Hartl D. Anuclear neutrophils keep hunting. Nat Med 2012; 18:1336-8.
575 17. Miller LS, Cho JS. Immunity against Staphylococcus aureus cutaneous infections. Nat Rev
576 Immunol 2011; 11:505-18.
577 18. Wang H, El Maadidi S, Fischer J, Grabski E, Dickhofer S, Klimosch S, et al. A frequent
578 hypofunctional IRAK2 variant is associated with reduced spontaneous hepatitis C virus
579 clearance. Hepatology 2015.
580 19. Bartok E, Bauernfeind F, Khaminets MG, Jakobs C, Monks B, Fitzgerald KA, et al. iGLuc: a
581 luciferase-based inflammasome and protease activity reporter. Nat Methods 2013; 10:147-
582 54.
583 20. Ito M, Shichita T, Okada M, Komine R, Noguchi Y, Yoshimura A, et al. Bruton's tyrosine kinase
584 is essential for NLRP3 inflammasome activation and contributes to ischaemic brain injury.
585 Nat Commun 2015; 6:7360.
586 21. Franklin BS, Bossaller L, De Nardo D, Ratter JM, Stutz A, Engels G, et al. The adaptor ASC has
587 extracellular and 'prionoid' activities that propagate inflammation. Nat Immunol 2014;
588 15:727-37.
589 22. Stutz A, Horvath GL, Monks BG, Latz E. ASC speck formation as a readout for inflammasome
590 activation. Methods Mol Biol 2013; 1040:91-101.

ACCEPTED MANUSCRIPT

591 23. Khan WN, Alt FW, Gerstein RM, Malynn BA, Larsson I, Rathbun G, et al. Defective B cell
592 development and function in Btk-deficient mice. Immunity 1995; 3:283-99.
593 24. de Almeida L, Khare S, Misharin AV, Patel R, Ratsimandresy RA, Wallin MC, et al. The PYRIN
594 Domain-only Protein POP1 Inhibits Inflammasome Assembly and Ameliorates Inflammatory
595 Disease. Immunity 2015; 43:264-76.
596 25. Pimienta G, Chaerkady R, Pandey A. SILAC for global phosphoproteomic analysis. Methods
597 Mol Biol 2009; 527:107-16, x.
598 26. Di Paolo JA, Huang T, Balazs M, Barbosa J, Barck KH, Bravo BJ, et al. Specific Btk inhibition
599 suppresses B cell- and myeloid cell-mediated arthritis. Nat Chem Biol 2011; 7:41-50.
600 27. Katsnelson MA, Rucker LG, Russo HM, Dubyak GR. K+ efflux agonists induce NLRP3
601 inflammasome activation independently of Ca2+ signaling. J Immunol 2015; 194:3937-52.
602 28. Tomlinson MG, Kane LP, Su J, Kadlecek TA, Mollenauer MN, Weiss A. Expression and function
603 of Tec, Itk, and Btk in lymphocytes: evidence for a unique role for Tec. Mol Cell Biol 2004;
604 24:2455-66.
605 29. Hornung V, Bauernfeind F, Halle A, Samstad EO, Kono H, Rock KL, et al. Silica crystals and
606 aluminum salts activate the NALP3 inflammasome through phagosomal destabilization. Nat
607 Immunol 2008; 9:847-56.
608 30. Holzinger D, Gieldon L, Mysore V, Nippe N, Taxman DJ, Duncan JA, et al. Staphylococcus
609 aureus Panton-Valentine leukocidin induces an inflammatory response in human phagocytes
610 via the NLRP3 inflammasome. J Leukoc Biol 2012; 92:1069-81.
611 31. Melehani JH, James DB, DuMont AL, Torres VJ, Duncan JA. Staphylococcus aureus Leukocidin
612 A/B (LukAB) Kills Human Monocytes via Host NLRP3 and ASC when Extracellular, but Not
613 Intracellular. PLoS Pathog 2015; 11:e1004970.
614 32. Takeuchi O, Hoshino K, Akira S. Cutting edge: TLR2-deficient and MyD88-deficient mice are
615 highly susceptible to Staphylococcus aureus infection. J Immunol 2000; 165:5392-6.
616 33. Cho JS, Guo Y, Ramos RI, Hebroni F, Plaisier SB, Xuan C, et al. Neutrophil-derived IL-1beta is
617 sufficient for abscess formation in immunity against Staphylococcus aureus in mice. PLoS
618 Pathog 2012; 8:e1003047.
619 34. Rieber N, Gavrilov A, Hofer L, Singh A, Oz H, Endres T, et al. A functional inflammasome
620 activation assay differentiates patients with pathogenic NLRP3 mutations and symptomatic
621 patients with low penetrance variants. Clinical Immunology 2015; 157:56-64.
622 35. Jefferies CA, Doyle S, Brunner C, Dunne A, Brint E, Wietek C, et al. Bruton's tyrosine kinase is
623 a Toll/interleukin-1 receptor domain-binding protein that participates in nuclear factor
624 kappaB activation by Toll-like receptor 4. J Biol Chem 2003; 278:26258-64.
625 36. Brunner C, Muller B, Wirth T. Bruton's Tyrosine Kinase is involved in innate and adaptive
626 immunity. Histology and histopathology 2005; 20:945-55.
627 37. Block H, Zarbock A. The role of the tec kinase Bruton's tyrosine kinase (Btk) in leukocyte
628 recruitment. Int Rev Immunol 2012; 31:104-18.
629 38. Coll RC, Robertson AA, Chae JJ, Higgins SC, Munoz-Planillo R, Inserra MC, et al. A small-
630 molecule inhibitor of the NLRP3 inflammasome for the treatment of inflammatory diseases.
631 Nat Med 2015; 21:248-55.
632 39. Teocchi MA, Domingues Ramalho V, Abramczuk BM, D'Souza-Li L, Santos Vilela MM. BTK
633 mutations selectively regulate BTK expression and upregulate monocyte XBP1 mRNA in XLA
634 patients. Immun Inflamm Dis 2015; 3:171-81.
635 40. Gaidt MM, Ebert TS, Chauhan D, Schmidt T, Schmid-Burgk JL, Rapino F, et al. Human
636 Monocytes Engage an Alternative Inflammasome Pathway. Immunity 2016; 44:833-46.
637 41. Duewell P, Kono H, Rayner KJ, Sirois CM, Vladimer G, Bauernfeind FG, et al. NLRP3
638 inflammasomes are required for atherogenesis and activated by cholesterol crystals. Nature
639 2010; 464:1357-61.
640 42. Halle A, Hornung V, Petzold GC, Stewart CR, Monks BG, Reinheckel T, et al. The NALP3
641 inflammasome is involved in the innate immune response to amyloid-beta. Nature
642 immunology 2008; 9:857-65.

ACCEPTED MANUSCRIPT

643 43. Murthy P, Durco F, Miller-Ocuin JL, Takedai T, Shankar S, Liang X, et al. The NLRP3
644 inflammasome and Bruton's tyrosine kinase in platelets co-regulate platelet activation,
645 aggregation, and in vitro thrombus formation. Biochem Biophys Res Commun 2016.

ACCEPTED MANUSCRIPT

Figure 1

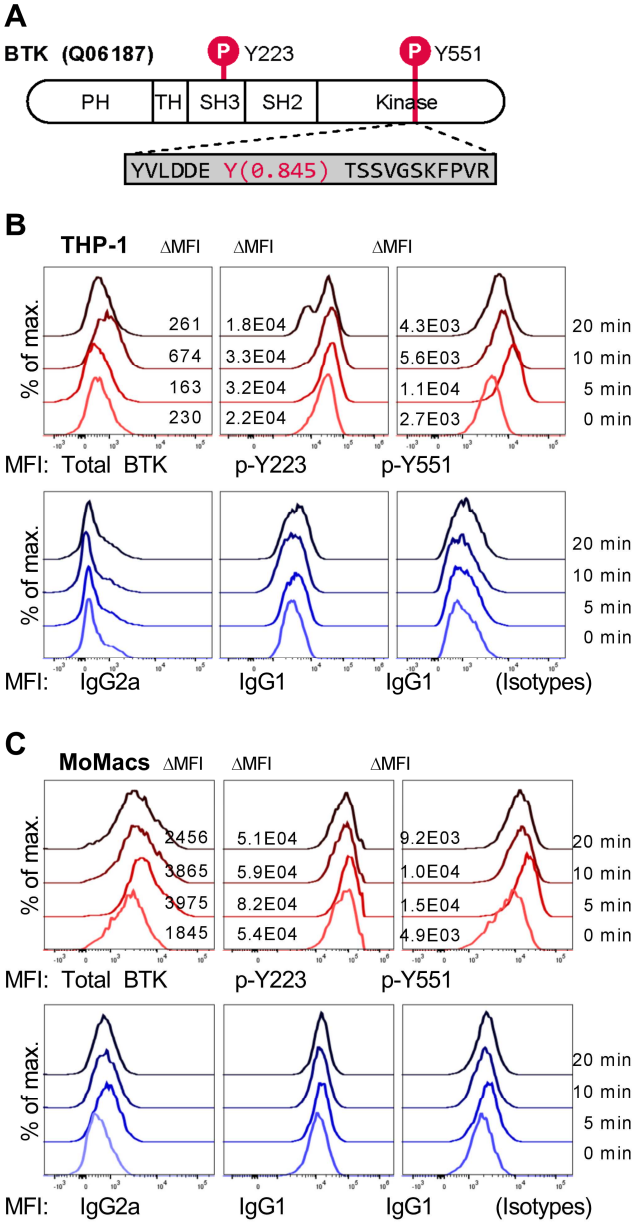
A
BTK (Q06187)
P Y223
P Y551
PH
TH
SH3
SH2
Kinase
YVLDDE Y(0.845) TSSVGSKFPVR
B
THP-1
ΔMFI
ΔMFI
ΔMFI
% of max.
261
674
163
230
1.8E04
3.3E04
3.2E04
2.2E04
4.3E03
5.6E03
1.1E04
2.7E03
20 min
10 min
5 min
0 min
MFI: Total BTK
p-Y223
p-Y551
IgG2a
IgG1
IgG1
(Isotypes)
C
MoMacs
2456
3865
3975
1845
5.1E04
5.9E04
8.2E04
5.4E04
9.2E03
1.0E04
1.5E04
4.9E03

Figure 2

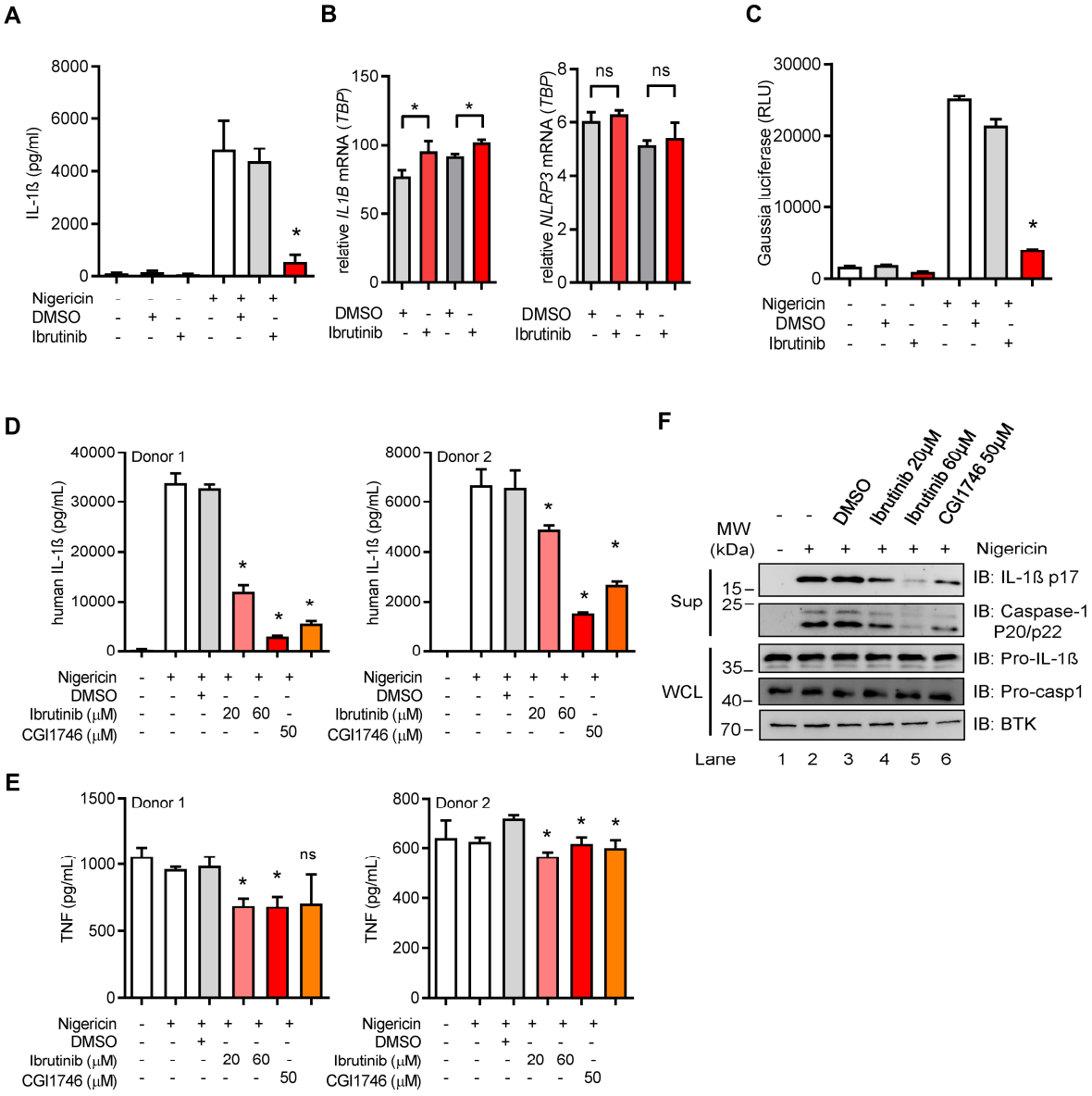
A
IL-1ß (pg/ml)
Nigericin
DMSO
Ibrutinib
B
relative IL1B mRNA (TBP)
relative NLRP3 mRNA (TBP)
ns
DMSO
Ibrutinib
C
Gaussia luciferase (RLU)
Nigericin
DMSO
Ibrutinib
D
Donor 1
Donor 2
human IL-1ß (pg/mL)
Nigericin
DMSO
Ibrutinib (µM)
CGI1746 (µM)
E
Donor 1
Donor 2
TNF (pg/mL)
ns
Nigericin
DMSO
Ibrutinib (µM)
CGI1746 (µM)
F
DMSO
Ibrutinib 20µM
Ibrutinib 60µM
CGI1746 50µM
MW (kDa)
Nigericin
Sup
WCL
IB: IL-1ß p17
IB: Caspase-1 P20/p22
IB: Pro-IL-1ß
IB: Pro-casp1
IB: BTK
Lane

Figure 3

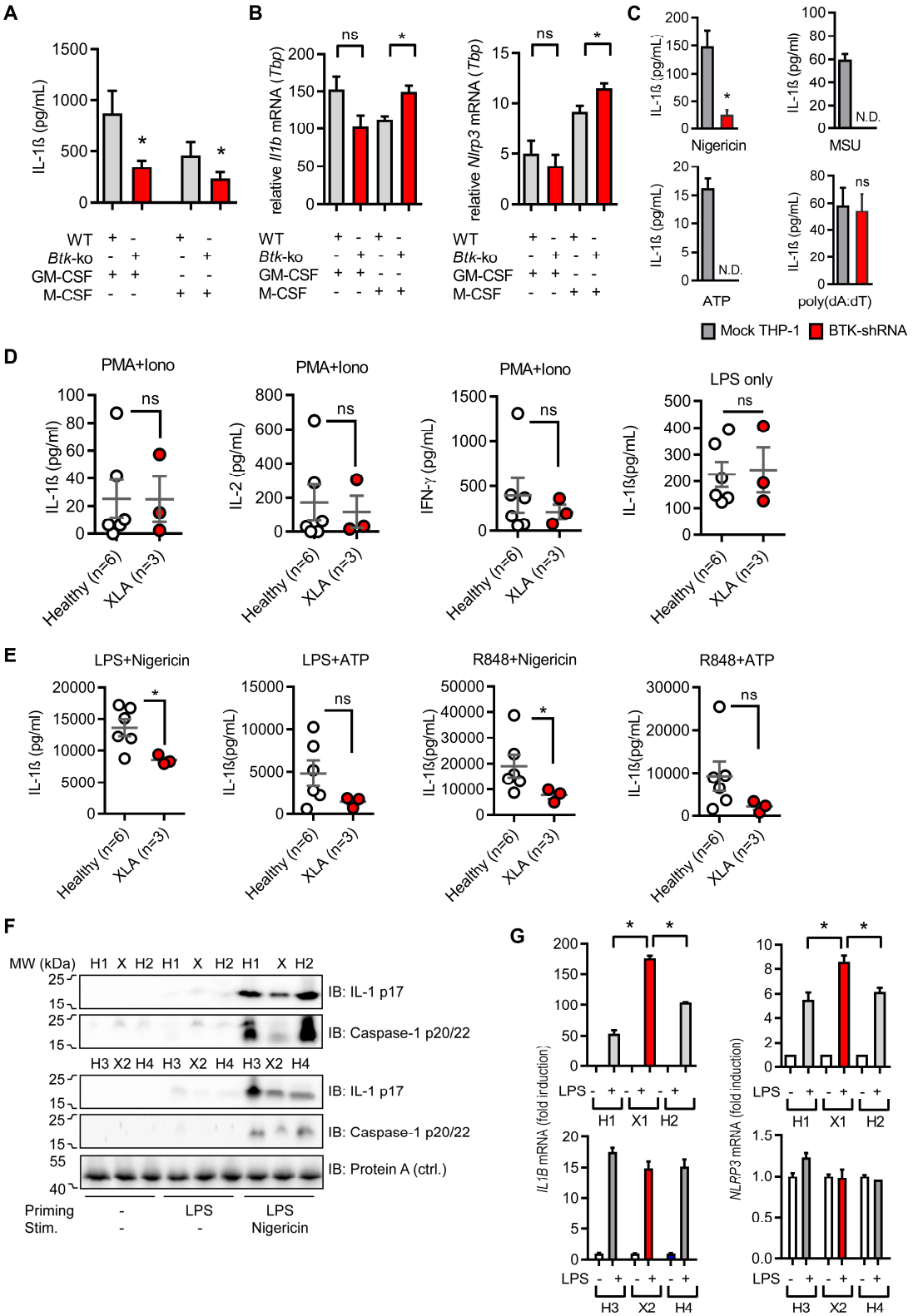
A
IL-1ß (pg/mL)
WT
Btk-ko
GM-CSF
M-CSF
B
relative Il1b mRNA (Tbp)
relative Nlrp3 mRNA (Tbp)
ns
*
C
IL-1ß (pg/mL)
Nigericin
MSU
ATP
poly(dA:dT)
N.D.
Mock THP-1
BTK-shRNA
D
PMA+Iono
LPS only
IL-1ß (pg/ml)
IL-2 (pg/mL)
IFN-γ (pg/mL)
Healthy (n=6)
XLA (n=3)
E
LPS+Nigericin
LPS+ATP
R848+Nigericin
R848+ATP
F
MW (kDa)
H1 X H2
H3 X2 H4
IB: IL-1 p17
IB: Caspase-1 p20/22
IB: Protein A (ctrl.)
Priming
Stim.
LPS
Nigericin
G
IL1B mRNA (fold induction)
NLRP3 mRNA (fold induction)
LPS
H1 X1 H2
H3 X2 H4

Figure 4

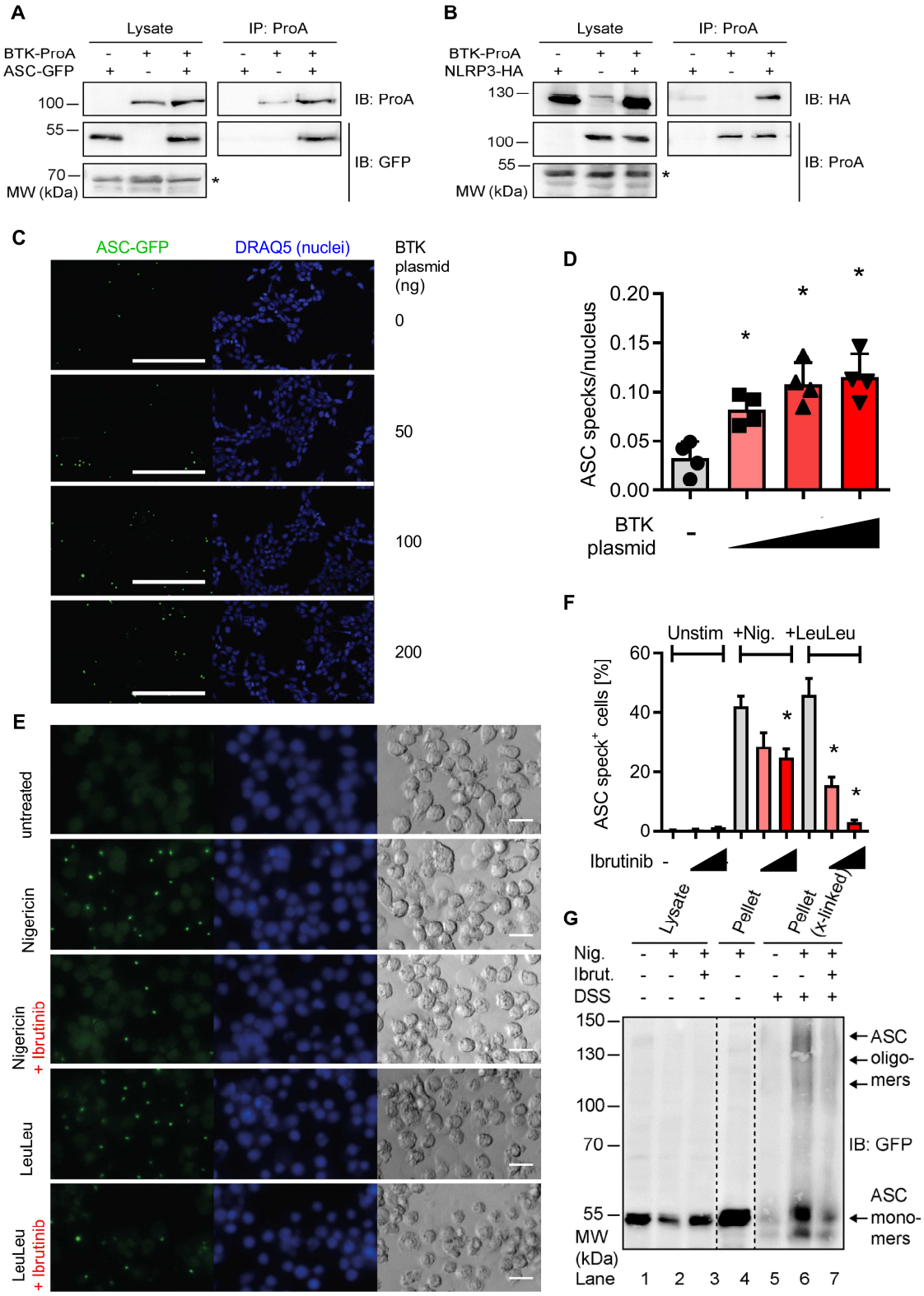
A
Lysate
IP: ProA
BTK-ProA
ASC-GFP
100
55
70
MW (kDa)
IB: ProA
IB: GFP
B
Lysate
IP: ProA
BTK-ProA
NLRP3-HA
130
100
55
MW (kDa)
IB: HA
IB: ProA
C
ASC-GFP
DRAQ5 (nuclei)
BTK plasmid (ng)
0
50
100
200
D
ASC specks/nucleus
0.20
0.15
0.10
0.05
0.00
BTK plasmid
E
untreated
Nigericin
Nigericin + Ibrutinib
LeuLeu
LeuLeu + Ibrutinib
F
Unstim
+Nig.
+LeuLeu
ASC speck+ cells [%]
60
40
20
0
Ibrutinib
G
Lysate
Pellet
Pellet (x-linked)
Nig.
Ibrut.
DSS
150
130
100
70
55
MW (kDa)
Lane
1 2 3 4 5 6 7
ASC oligo-mers
IB: GFP
ASC mono-mers

Figure 5

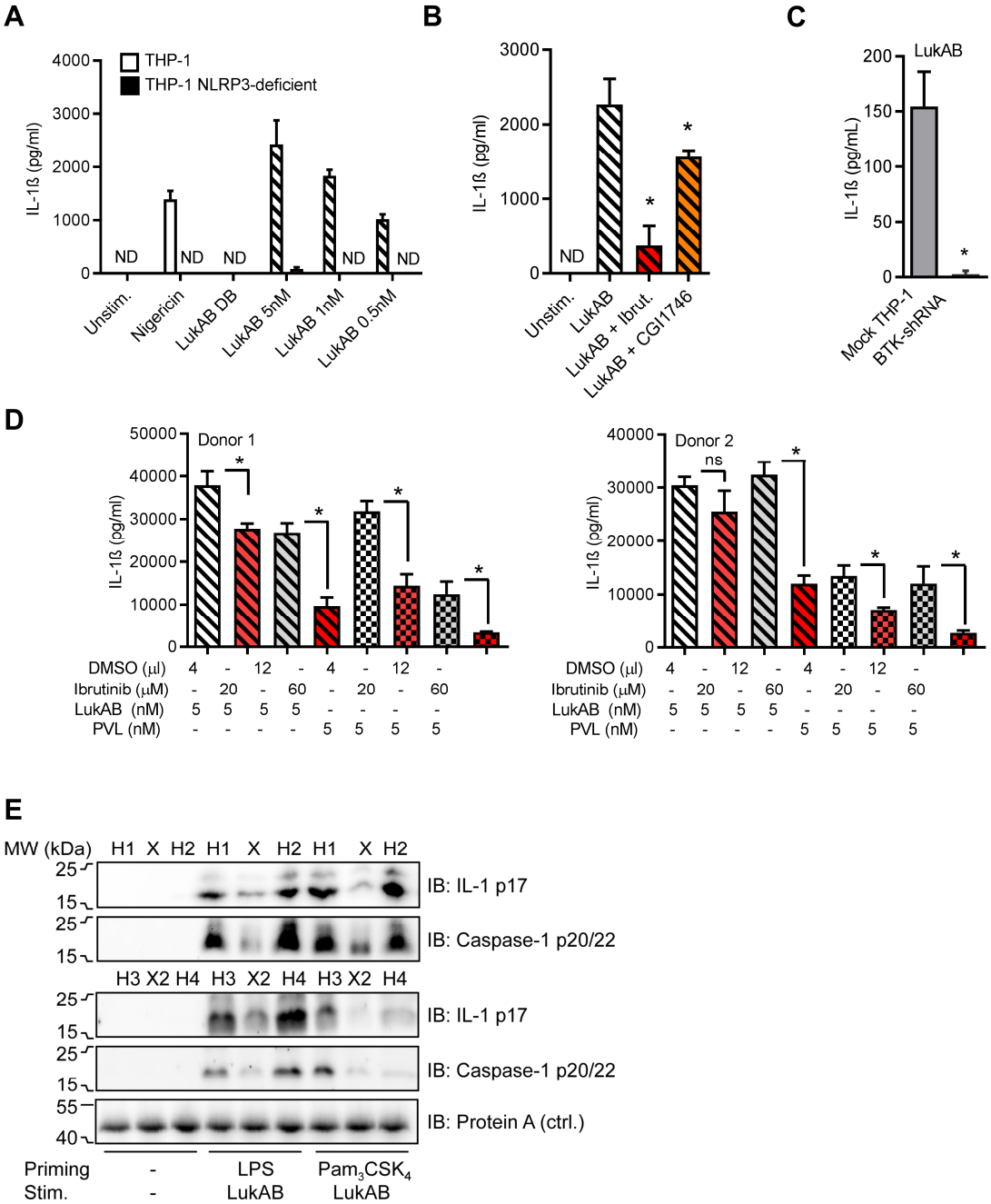
A
THP-1
THP-1 NLRP3-deficient
IL-1ß (pg/ml)
ND
Unstim.
Nigericin
LukAB DB
LukAB 5nM
LukAB 1nM
LukAB 0.5nM
B
IL-1ß (pg/ml)
Unstim.
LukAB
LukAB + Ibrut.
LukAB + CGI1746
C
LukAB
IL-1ß (pg/mL)
Mock THP-1
BTK-shRNA
D
Donor 1
Donor 2
IL-1ß (pg/ml)
ns
DMSO (µl)
Ibrutinib (µM)
LukAB (nM)
PVL (nM)

E
MW (kDa)
H1 X H2 H1 X H2 H1 X H2
IB: IL-1 p17
IB: Caspase-1 p20/22
H3 X2 H4 H3 X2 H4 H3 X2 H4
IB: IL-1 p17
IB: Caspase-1 p20/22
IB: Protein A (ctrl.)
Priming - LPS Pam3CSK4
Stim. - LukAB LukAB

Figure 6

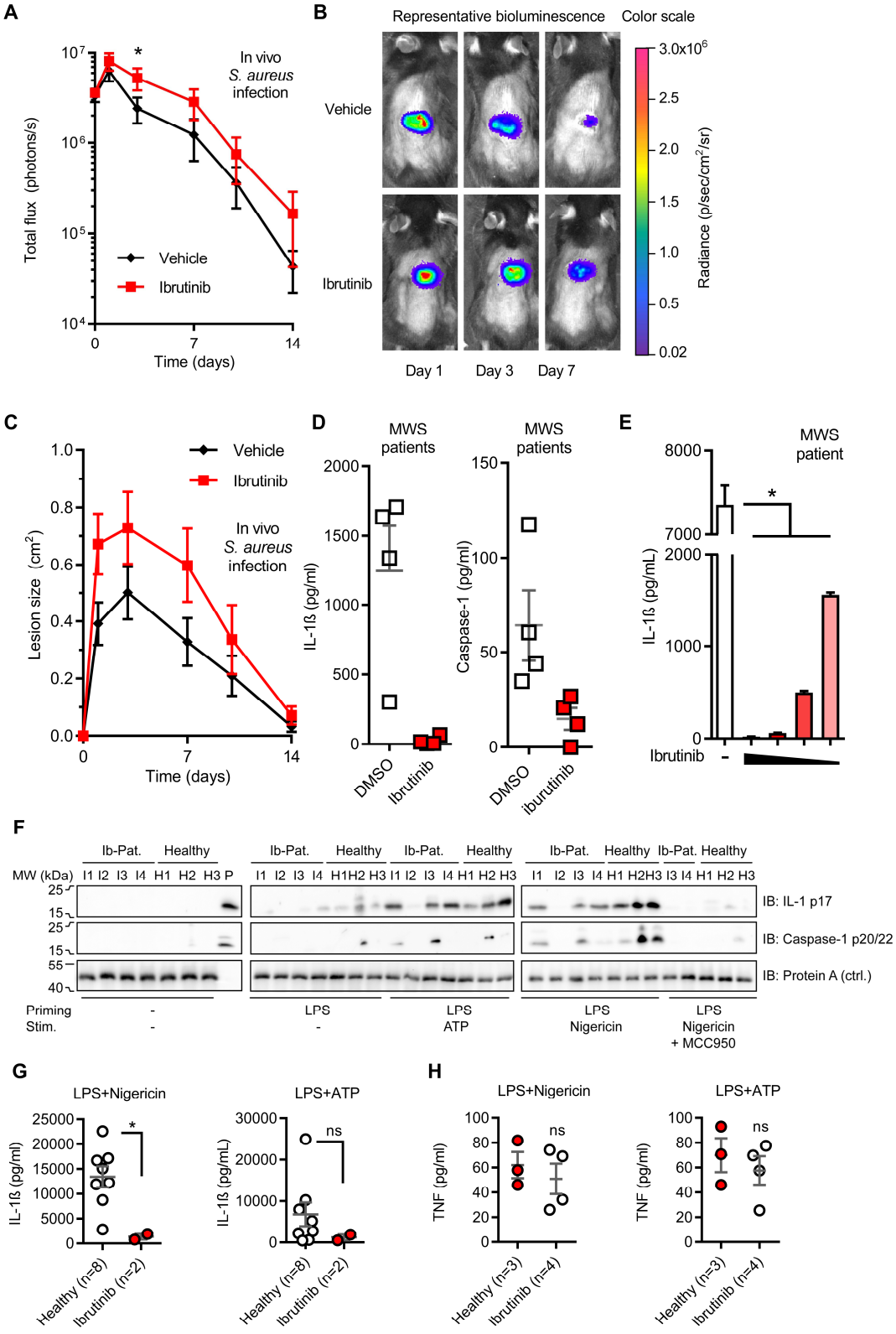
A
In vivo
S. aureus
infection
Total flux (photons/s)
Time (days)
Vehicle
Ibrutinib
B
Representative bioluminescence
Color scale
Vehicle
Ibrutinib
Day 1
Day 3
Day 7
Radiance (p/sec/cm²/sr)
C
Lesion size (cm²)
Time (days)
D
MWS patients
IL-1ß (pg/ml)
Caspase-1 (pg/ml)
DMSO
Ibrutinib
iburutinib
E
MWS patient
IL-1ß (pg/mL)
Ibrutinib
F
Ib-Pat.
Healthy
MW (kDa)
IB: IL-1 p17
IB: Caspase-1 p20/22
IB: Protein A (ctrl.)
Priming
Stim.
LPS
ATP
Nigericin
LPS Nigericin + MCC950
G
LPS+Nigericin
LPS+ATP
IL-1ß (pg/ml)
IL-1ß (pg/mL)
Healthy (n=8)
Ibrutinib (n=2)
H
TNF (pg/ml)
Healthy (n=3)
Ibrutinib (n=4)
ns

ACCEPTED MANUSCRIPT

Human NLRP3 inflammasome activity is regulated by and potentially targetable via BTK

Authors

Xiao Liu[a] MSc, Tica Pichulik[a] PhD MSc, Olaf-Oliver Wolz[a] PhD MSc, Truong-Minh Dang[a] PhD MSc, Andrea Stutz[b] MSc, Carly Dillen[c] PhD MSc, Magno Delmiro Garcia[a] MSc, Helene Kraus[d] MD, Sabine Dickhöfer[a] MTA, Ellen Daiber[e] Dipl Biol, Lisa Münzenmayer[e] MSc, Silke Wahl[f] PhD MSc, Nikolaus Rieber[g] MD, Jasmin Kümmerle-Deschner[g] MD, Amir Yazdi[h] MD, Mirita Franz-Wachtel[f] PhD MSc, Boris Macek[f] PhD MSc, Markus Radsak[i] MD, Sebastian Vogel[j] MD, Berit Schulte[e] MD, Juliane Sarah Walz[k] MD, Dominik Hartl[g] Prof. PhD MD, Eicke Latz[b,l] Prof. PhD MD, Stephan Stilgenbauer[m] Prof. PhD MD, Bodo Grimbacher[d] Prof. PhD MD, Lloyd Miller[c] PhD MD, Cornelia Brunner[n] Prof. PhD MSc, Christiane Wolz[e] Prof. PhD MSc, Alexander N. R. Weber[a]* Prof. PhD MPhil.

Supplemental figure legends

Figure S1: Whole blood analysis of XLA and healthy donors. Prior to PBMC purification, whole blood from the 3 XLA and 6 healthy donors shown in Fig. 3C,D was stained using anti-CD3-FITC and anti-CD19-Pacific blue monoclonal Abs and analyzed by flow cytometry as indicated.

Figure S2: BTK localizes around ASC specks and CGI1746 blocks ASC speck formation. (A) HEK293T cells were transfected with BTK-HA and ASC-GFP plasmids, fixed with methanol 48 h later, nucleic acids stained with To-pro-3 and samples analyzed by confocal microscopy. Z-stacks from two fields of view from at least three experiments are shown. Scale bar = 20 µm. (B) Quantification of ASC specks of immortalized *Nlrp3* KO macrophages overexpressing NLRP3-FLAG and ASC-mCerulean treated with CGI1746 at 50 µM or solvent control (-) for 60 min before stimulation with 1 mM Leu-Leu-OMe·HCl for 90 min. Cells were fixed after stimulation and nucleic acids stained with DRAQ5. Quantification was performed on ten fields per condition using CellProfiler and shows mean percentage of cells with ASC specks from n=2 experiments ± SEM. A Student's *t*-test was used.

Figure S3: LukAB and PVL dose-dependently activate NLRP3-dependent IL-1β release in THP-1 cells and primary MoMacs. Human primary MoMacs were primed with 300 ng/ml LPS for 3 h, and then stimulated with the indicated amounts of LukAB, PVL, Nigericin or dialysis buffer for 60 min. IL-1β in the supernatant was quantified by triplicate ELISA (mean +SD). R = out of range. One representative of two identical experiments shown.

Figure S4: BTK inhibition negatively affects IL-1β-dependent *S. aureus* clearance *in vivo.* C57BL/6 mice (n=10 per group) received three consecutive i.v. injections of vehicle or ibrutinib on days -1,0 and 1 followed by one topical ibrutinib application on day 2. Inhibitor and vehicle-treated mice were inoculated intradermally with a bioluminescent community-acquired MRSA strain (USA300 LAC::*lux*). At the indicated days, mean total lesion size (cm^2) was measured and representative skin lesions are shown.

Figure S5: The NLRP3 inhibitor, MCC950, reduces IL-1 and caspase-1 processing further in XLA patients. (A) LPS-primed PBMC from a male XLA patient and age-matched male healthy donors (n=2) were treated with 15 µM Nigericin for 1 h in the presence of absence of 1 µM MCC950. IL-1β was quantified by ELISA (mean ±SD of technical). (B) Stimulated PBMC were also analyzed by immunoblot using anti-IL-1β p17 or -caspase-1 p20/p22 specific Abs.

Figure S6: Excessive IL-1β and caspase-1 release in MWS patients in response to only LPS. PBMC from MWS patients (n=4) and healthy donors (n=6) were treated with LPS only for 4 h. IL-1β and caspase-1 release was quantified by ELISA (mean ±SEM of biological replicates, each symbol represents one donor).

ACCEPTED MANUSCRIPT

Supplemental Experimental Procedures

Reagents. Nigericin, LPS, PMA and Ionomycin were from Invivogen, ATP from Sigma, ibrutinib from Selleckchem, CGI1746 from Selleckchem, recombinant GM-CSF for monocyte differentiation from Prepro-Tech, Ficoll from Merck Millipore, anti-CD14-PE from BD. Abs for immunoblot were as follows: Caspase-1 (D7F10) Abs from Cell Signaling Technology, ASC (F-9) from Santa Cruz, IL-1β from R&D and BTK from BD. For flow cytometry, anti-CD11b-APC and anti-CD14-PE were from ImmunoTools, anti-CD19-Pacific Blue from Biolegend, anti-CD3-FITC from BD, anti-Btk (pY551)-PE, anti-Btk (pY223)-Alexa Fluor 647 were from BD. For co-IP experiments all primary antibodies were purchased from Sigma-Aldrich: Anti-HA (H9658) and anti-GFP (G1544) both used 1:5000 and anti-Protein A (P3775, dilution 1:62,500). Secondary HRP-coupled antibodies were anti-mouse (Thermo Fisher Scientific PA1-86015) and anti-rabbit (Cell Signaling Technology 5127). For the DSS-crosslinking anti-ASC (Santa Cruz Biotechnology sc-271054) was used. Recombinant Protein was from Thermo scientific.

Study subjects and sample acquisition. All human subjects provided written informed consent in accordance with the Declaration of Helsinki and the study was approved by the local ethics committees. Buffy coats from healthy donors were provided by the Tübingen University Hospital Transfusion Medicine Department. Male XLA patients with confirmed genetic and clinical BTK deficiency were recruited at the Center for Immunodeficiency at Freiburg University Hospital. Male healthy donors in a similar age range were recruited at the Department of Immunology, Tübingen, and blood taken on the same day as that from the XLA patients. Samples were processed in the same way and measured together. MWS patients were recruited at the Pediatrics Department of the University Hospital Tübingen as described [1]. Patients are described in detail below.

Isolation and stimulation of primary immune cells. PBMC were isolated from whole blood or buffy coats using Ficoll density gradient purification and washed three times with RPMI to remove residual platelets and then seeded in RPMI-1640 (Sigma), 10 % FBS (GE Healthcare), 2 mM L-Glutamine (Life technologies), 1 % Pen Strep (Life technologies). PBMC were isolated from peripheral blood of 3 XLA patients and 6 healthy donors. Cells were then treated with 10 ng/ml LPS for 3 h, and 15 µM Nigericin for 1 h, or instead with 50 ng/ml PMA and 1 µM Ionomycin for 4 h. PBMC from MWS were seeded at a concentration of $1x10^6$ cells/ml in 24-well tissue culture plates. Cells were then treated with 10 ng/ml LPS, 1 mM ATP concomitantly with 60 µM ibrutinib or a DMSO control for 4 h and supernatants collected for ELISA. For macrophage differentiation, monocytes were purified by positive selection from PBMC using anti-CD14 magnetic beads (Miltenyi Biotec, >90% purity assessed by anti-CD14-PE flow cytometry) and seeded at a concentration of $1x10^6$ cells/ml in 96-well tissue culture plates. Cells were differentiated into macrophages in the presence of 25 ng/ml recombinant human GM-CSF for 5 days [2]. Monocyte-derived macrophages were then primed with 300 ng/ml LPS for 3 h and pre-treated with ibrutinib at 20µM or 60µM for 10 min before stimulation with 15 µM Nigericin or the indicated amounts of LukAB or PVL for 1 h. In all cases, supernatants were then collected for ELISA.

Plasmid constructs. ASC, NLRP3 and BTK coding sequences in pENTR clones were from the genomics core facility at DKFZ Heidelberg, German. The inserts were transferred into pDEST plasmids containing N-terminal streptavidin-hemagglutinin (NLRP3) (T. Bürckstümmer, CeMM, Vienna and M. Gstaiger, ETH Zurich), and C-terminal Protein A (M. Kögl, DKFZ Heidelberg) or GFP tags (Stefan Pusch, Neuropathology, Heidelberg University) by LR Gateway cloning (Invitrogen). Correct transfer was checked by restriction digest and DNA sequencing.

Cell culture. HEK293T cells were cultured in DMEM supplemented with 10% fetal calf serum, L-glutamine (2 mM), penicillin (100 U/ml), streptomycin (100 µg/ml) (all from Life Technologies). THP-1 (ATCC) cells were cultured in RPMI 1640 supplemented with 10% fetal calf serum, L-glutamine (2 mM), penicillin (100 U/ml), streptomycin (100 µg/ml)(all from Life Technologies). THP-1 Null (stably expressing a non-targeting shRNA) and NLRP3-deficient (stably expressing an NLRP3-targeting shRNA, both from Invivogen) were cultured in RPMI 1640 supplemented with 10% fetal calf serum, L-

ACCEPTED MANUSCRIPT

glutamine (2 mM), penicillin (100 U/ml), streptomycin (100 µg/ml) (all from Life Technologies), Sodium pyruvate (1 mM) from Invitrogen, HEPES buffer (10 mM) from Sigma, Normocin (100 µg/ml) from Invivogen, Hygromycin B (100 µg/ml) from Invitrogen. iGluc THP-1 cells were a kind gift of V. Hornung, Institute of Molecular Medicine, Munich and cultured as described [3]. BTK-shRNA- and mock control-THP-1 cells were a kind gift of R. Morita, Keio University School of Medicine, Tokyo and were cultured in RPMI 1640 supplemented with 10% fetal calf serum, L-glutamine (2 mM), penicillin (100 U/ml), streptomycin (100 µg/ml) (all from Life Technologies), in the presence of 1.5 and 2 mg/ml G418, respectively. ASC-mCerulean expressing immortalized macrophages or THP-1 cells were described previously [4, 5]. All cell lines and primary cells were cultured at 37 °C and 5% CO_2.

Mice and generation of BMDM. *Btk* KO mice have been described previously [6]. Btk KO and wild type littermates (all C57BL/6 background) were used at an age of 8 to 12 weeks. In brief, BM cells were isolated from femurs and tibiae using standard procedures (details available on request) and $3x10^6$ cells/ml plated in 10 cm non-tissue culture coated dishes in 10 ml complete RPMI media containing 10% GM-CSF (M1 polarization) or M-CSF (M2 polarization) conditioned medium for 5-7 days. Cells were always counted and re-seeded prior to *in vitro* assays to ensure equal cell numbers. *Ex vivo* animal experiments (Fig. 3 A, B) were in accordance with institutional guidelines and German animal protection laws. *In vivo* infection experiments (Fig. 6) were approved by the Johns Hopkins University Animal Care and Use Committee (ACUC Protocol NO. MO15M421). C57BL/6 female mice at 8 weeks of age were obtained from Jackson Laboratories (Bar Harbor, ME). All mouse colonies were maintained in specific-pathogen free conditions.

Mass spectrometry analysis. THP-1 Null cells (Invitrogen) were grown in "light" (L-lysine/Lys0, L-arginine/Arg0), "medium-heavy" (D4-L-lysine/Lys4, ^{13}C6-L-arginine/Arg6) and "heavy" ($^{13}C_6{}^{15}N_2$-L-lysine/Lys8, ^{13}C6^{15}N4-arginine/Arg10) SILAC medium for three passages. Incorporation of the labeled amino acids was in each case confirmed to be over 97%. For the experiment cells were primed with 300 ng/ml PMA for three hours and left to rest overnight. The next day the cells were detached and either left unstimulated (light) or stimulated with 15 µM Nigericin for 5 minutes (medium) or 10 minutes (heavy). After washing with ice-cold PBS (containing phosphatase and protease inhibitors, Roche), cells pellets were snap-frozen and stored at -80 °C prior to analysis. For phosphopeptide enrichment cells were lysed in denaturation buffer (6M Urea, 2M thiourea in 10 mM Tris buffer, pH 8.0) and DNA was removed by addition of benzonase. After determining the amount of protein in the lysates using a Bradford assay, 3 mg protein of each condition were pooled and the mixture was digested in solution with trypsin. The resulting peptide mixture was subjected to phosphopeptide enrichment as described previously [7], with minor modifications: Peptides were separated by strong cation exchange (SCX) chromatography with a gradient of 0 to 35% SCX solvent B resulting in eight fractions that were subjected to phosphopeptide enrichment by TiO_2 beads. Elution from the beads was performed three times with 100 µl of 40% ammonia hydroxide solution in 60% acetonitrile (pH > 10.5). Peptide-rich fractions were subjected to TiO2 enrichment multiple times. Enrichment of phosphopeptides from the SCX flow-through was done in five cycles. LC-MS/MS analyses were performed on an EasyLC nano-HPLC (Proxeon Biosystems) coupled to an LTQ Orbitrap XL (Thermo Scientific) as described previously [8]. The peptide mixtures were injected onto the column in HPLC solvent A (0.5% acetic acid) at a flow rate of 500 nl/min and subsequently eluted with a 127-min (phosphoproteome) segmented gradient of 5–33-90% HPLC solvent B (80% ACN in 0.5% acetic acid). During peptide elution the flow rate was kept constant at 200 nl/min. The five most intense precursor ions were fragmented by multistage activation of neutral loss ions at -98, -49, and -32.6 Th relative to the precursor ion [9]. Sequenced precursor masses were excluded from further selection for 90 s. Full scans were acquired at resolution of 60,000 (Orbitrap XL). The target values were set to 5000 charges for the LTQ (MS/MS) and 10^6 charges for the Orbitrap (MS), respectively; the maximum allowed fill times were 150ms (LTQ) and 1000 ms (Orbitrap). The lock mass option was used for real time recalibration of MS spectra [7]. The MS data were processed using default parameters of the MaxQuant software (v1.2.2.9) [10]. Extracted peak lists were submitted to database search using the Andromeda search engine [11] to query a target-decoy [12] database of *H. sapiens* proteome (downloaded from Uniprot on the 25 December 2012), containing in addition 248 commonly

ACCEPTED MANUSCRIPT

observed contaminants. In database search, full tryptic specificity was required and up to two missed cleavages were allowed. Carbamidomethylation of cysteine was set as fixed modification; protein N-terminal acetylation, oxidation of methionine, and phosphorylation of serine, threonine, and tyrosine were set as variable modifications. Initial precursor mass tolerance was set to 6 ppm at the precursor ion and 0.5 Da at the fragment ion level. False discovery rates were set to 1% at peptide, phosphorylation site, and protein group level. Details regarding other phospho-peptides with Nigericin-dependent are available upon request.

ELISA. IL-1ß, IL-2, TNF and IFNγ in supernatants were determined using half-area plates by ELISA (Biolegend) using triplicate points on a standard plate reader.

RT qPCR. mRNA was isolated using the RNeasy Mini Kit on a Qiacube robot (both Qiagen), transcribed to cDNA (High Capacity RNA-to-cDNA Kit; LifeTechnologies) and *IL1b, Nlrp3, IL1 and NLRP3* mRNA expression quantified relative to TBP using TaqMan primers (LifeTechnologies) on a real-time cycler (Applied Biosystems; 7500 fast) as described in [13]. Comparable CT values for TBP (not shown) in all treatment groups confirmed equal cell numbers.

ASC speck formation assay and confocal microscopy. $4x10^4$ HEK293T cells were plated (24-well format, Greiner Bio One) and transiently transfected as indicated. 48 hours later, cells were fixed with 100% methanol, nucleic acids were stained with To-pro-3 (Thermo Fisher), and BTK-HA stained using anti-HA-Alexa 594-conjugated antibodies. Samples were analyzed using a Zeiss LSM 510 confocal microscope under the 20x objective. Excitation and emission wavelengths are available on request. Nuclei and ASC-GFP particles counting and analysis were performed with the ImageJ software, further details on request. Immortalized *Nlrp3* KO macrophages overexpressing NLRP3-FLAG and ASC-mCerulean were pretreated with ibrutinib or solvent control for 10 min before stimulation (or with CGI1746 or solvent control) for 60 min before stimulation with either 5 µM Nigericin (Life Technologies) or 1 mM Leu-Leu-OMe▪HCl (Chem-Impex) for 90 min. After stimulation, cells were fixed with 4% formaldehyde and nucleic acids were stained with DRAQ5 (eBioscience). Cells were imaged with a Zeiss Observer.Z1 epifluorescence microscope using a 20x objective as decribed [5]. The number of cells and the number of specks were counted for 10 images per condition using CellProfiler [14].

Pro-IL-1β and caspase-1 cleavage. To monitor caspase-1 and pro-IL-1β processing, equal numbers of cells were primed by PMA (100 ng/ml, Invivogen) overnight or LPS (300 ng/ml, Invivogen) for 3 hours, and then stimulated with indicated stimuli in Opti-MEM (Gibco). Protein in supernatants was precipitated by methanol (VWR International) and chloroform (Sigma). Where applicable, recombinant Protein A was added prior to precipitation as a control. Where applicable, the cell fractions were lysed in a RIPA buffer with protease inhibitors (Sigma). 15% and 12% SDS-PAGE gels were used for protein from supernatants and whole cell lysates, respectively, and probed with the indicated antibodies.

Co-immunoprecipitation. For co-immunoprecipitations, $1.5x10^6$ HEK293T were plated in 10 cm dishes (Greiner Bio One) and 2-6 hours later transfected using calcium phosphate precipitation method with 5 µg of appropriate plasmids. Cells were lysed 48 hours later in a buffer (50 mM Tris pH 8, 280 mM NaCl, 0.5% NP-40, 0.2 mM EDTA, 2 mM EGTA, 10% glycerol, 1 mM DTT) with protease/phosphatase inhibitors (Roche). Cleared lysates were stored for immunoblot analysis. The remainder was subjected to immunoprecipitation of the BTK-Protein A fusion protein, 30 µl of lysis buffer-equilibrated Dynabeads (M-280 Sheep Anti-Mouse IgG from Thermo Fisher Scientific) were incubated with the lysates at 4°C for 3 h. After 4x washing of precipitated protein-complexes, samples were boiled in Invitrogen's NuPAGE 4x LDS loading dye supplemented with 10x Sample Reducing Agent and applied for SDS-PAGE and immunoblot.

Crosslinking of ASC-oligomers. $2x10^6$ THP-1 null or ASC-mCerulean cells (Veit Hornung) were plated in 6 well format (Greiner Bio One), primed with 100 ng/ml PMA for overnight or with 300 ng/ml LPS for 2 hours, respectively, then treated with 60 µM ibrutinib for 1 hour and then with 15 µM Nigericin

ACCEPTED MANUSCRIPT

for 1 hour unless otherwise stated. After washing with PBS, cells were lysed at 4°C in 100 µl buffer [15] containing 20 mM HEPES pH 7.4, 100 mM NaCl, 1% NP-40, 1 mM sodium orthovanadate and supplemented with protease inhibitors (Roche) and Benzonase (Sigma-Aldrich). Lysates were cleared (16000xg, 4°C, 15 min) and used for immunoblot analysis. Pellets were resuspended in 250 µl PBS and subjected with 2 mM disuccinimydyl suberate (DSS, Thermo Scientific) for 1 h at room temperature. Crosslinked samples were spun (16000xg, 4°C, 15 min) and pelleted fraction resuspended and boiled in Invitrogen's NuPAGE LDS loading dye supplemented with Sample Reducing Agent and applied for immunoblot.

Flow cytometry and phospho-flow. For whole blood analysis of healthy donors and XLA patients 200 µl of whole blood from patients and health controls was stained with a mix of antibodies detecting cell surface antigens: anti-CD3-FITC, -CD19-Pacific Blue, -CD14-PE and -CD11b-APC for 30 minutes at room temperature in the dark. Samples were then fixed and permeabilized (Lyse/Fix Buffer, BD) for 20 minutes, washed and resuspended in 200µl of PBS 0.5% BSA for analysis (BD Fortessa). A standardized protocol and identical flow cytometer settings were used for all donors. Further settings on request. For phosflow analysis, the indicated primed cells were treated and then fixed (Lyse/Fix Buffer, BD). For phosflow analysis, the indicated primed cells were treated and then fixed (Lyse/Fix Buffer, BD). LIVE⁄DEAD Fixable Aqua was used to stain dead cells (Life Technologies). Cells were permeabilized with 1 ml of cold methanol, Fc-receptors were blocked (Human AB serum) and cells were stained with antibodies against anti-Btk (pY551) PE, anti-Btk (pY223) BV421, and anti-total BTK Alexa Fluor 647 (all from BD). Corresponding isotype controls were from Immunotools.

***S. aureus* strains.** For experiments in mice, a modified USA300 strain, LAC::*lux* [16], which possesses a modified *luxABCDE* operon from *Photohabdus luminescens* stably integrated into the bacterial chromosome that was transduced from bioluminescent strain Xen29 (PerkinElmer). Live and metabolically active USA300 LAC::*lux* bacteria constitutively emit a blue-green light, which is present in all progeny. USA300 strain LAC::*lux* was streaked onto a tryptic soy agar (TSA) plate (tryptic soy broth plus 1.5% bacto agar (BD Biosciences) and grown overnight at 37° C in an bacterial incubator. Single colonies were picked and placed into tryptic soy broth (TSB) and grown overnight in shaking culture in a 37° C shaker at 240 RPM. After overnight culture (18 hours), a 1:50 subculture in TSB was prepared for 2 hours at 37° C to achieve mid-logarithmic phase bacteria. The bacteria were pelleted, resuspended in sterile PBS, and washed 3 times. The absorbance (A_{600}) was measure to estimate the number of CFUs, which was verified after overnight culture on TSA plates.

***In vivo* infection model.** Ibrutinib (6 mg/kg)(Selleckchem) in 3% DMSO (Sigma-Aldrich) and 5% corn oil (Sigma-Aldrich) in PBS or vehicle control was injected i.v. via the retro-orbital vein in anesthetized mice on days -1, 0, 1. In addition, mice received one application of ibrutinib (6mg/kg) in 10 µL DMSO or vehicle control on day 2. For infection, the dorsal backs of anesthetized mice (2% isoflurane) were shaved and injected intradermally with $3x10^7$ CFU of *S. aureus* LAC::*Lux:* in 100 µL of PBS using a 29 gauge insulin syringe on day 0. Digital photographs were taken on days 1, 3, 7, 10 and 14 and total lesion size (cm^2) measurements were analyzed using Image J software (http://imagej.nih.gov/ij/) and a millimeter ruler as a reference.

Quantification of *in vivo S. aureus* bioluminescent imaging. Mice were anesthetized (2% isoflurane) and *in vivo* bioluminescent imaging was performed (Lumina III IVIS, PerkinElmer) and total flux (photons/s) within a circular region of interest measuring $1x10^3$ pixels was measured using Living Image software (PerkinElmer) (limit of detection: $2x10^4$ photons/s).

Purification of LukAB and PVL. The pQE30 vector (Qiagen) was used to produce recombinant His-tagged LukS-PV, LukF-PV, LukA and LukB (the 2 single components of PVL and LukAB, respectively) using the following oligonucleotides: LukF (BamlukF-for: GGGGGGATCCTCCAATACACTTGATGCAGCT and PstlukF-rev: GCGCCTGCAGTCTATCTGTTTAGCTCATAGGATT); LukS (BamHluk-S1: GGGGGGATCCAAAGCTGATAACAATATTGAGAA and Pstluk-S2: GGGGCTGCAGTCAATTATGTCCTTTCACTT); LukB (PstblhA-for:

ACCEPTED MANUSCRIPT

BCGCGCTGCAGGGCAACTTTTATTACTTATTTCTT and BamblhA-rev: CCCCGGATCCCCAGCTACTTCATTTGCAAAGATT); LukA (Pstblh-S 1: CCCCCTGCAGCGCCCTTTCAATATTATCCT and BamHblh-S2: CCCCGGATCCAATTCAGCTCATAAAGACTCTCAA) . Primers were chosen to omit the region predicted to encode the signal peptide. PCR fragments were cloned into the BamHI-PstI cloning site of pQE30. Plasmids were transformed in *E. coli* BL21 and verified by sequencing. LukS-PV, LukF-PV and LukA proteins were purified by affinity chromatography on nitrilotriacetic acid (Ni-NTA) columns (Qiagen) under native conditions according to the instruction of the manufacturer (Qiagen) using 50 mM NaH_2PO_4, 300 mM NaCl, 250 mM imidazole, 20 % glycerol for elution. LukB was purified under denaturing conditions from inclusion bodies. Briefly, inclusion bodies were re-suspended in 6M guanidine HCl, 20 mM Tris pH 8,0, 500 mM NaCl, 20 % glycerol, centrifuged and the supernatant packed with NI-NTA on columns. Columns were washed (6M guanidine HCl, 20 mM Tris pH 8,0, 500 mM NaCl, 20 % glycerol, 50 mM imidazole) and LukB eluted with 6M guanidine HCl, 20 mM Tris pH 8,0, 500 mM NaCl, 20 % glycerol, 300 mM imidazole. The fusion proteins were dialyzed against PBS/50 % glycerol and stored at -20°C until use. Endotoxin contamination of the toxin stock solutions was excluded using a limulus assay with a detection limit of 0.25 EU/ml (Lonza) and found negative. For use the single components were mixed in equal molar ratio. IL-1β secretion was not detectable in stimulations using the single components (not shown).

Data analysis and statistics. Data were imported into and analyzed in GraphPad Prism v.5.0 using two-tailed Student's *t*-tests and non-parametric Mann-Whitney-U or Wilcoxon matched-pairs signed rank test unless stated otherwise. A p-value of <0.05 was generally considered statistically significant and, even if considerably lower marked as * throughout.

XLA patient characteristics

All patients were adult males and provided written informed consent for participation in the study.

Patient 1 (Fig. 4DE,D) was diagnosed with XLA due to agammaglobulinemia and absence of B cells following recurring bronchopulmonary infections. A BTK mutation mapping to a splicing site was confirmed by sequencing (g.IVS17+5G>A, c.1750+5G>A).

Patient 2 (Fig. 4D,E) was diagnosed with XLA due to absence of all Ig subtypes and absence of B cells following recurring bronchopulmonary infections. A coding BTK mutation was confirmed by sequencing (c1361A>T, p.454H>L). The patient has been on IVIG since 1984.

Patient 3 (Fig. 4D,E) was diagnosed with XLA due to absence of all Ig subtypes and absence of B cells following recurring bronchopulmonary infections, episodes of pneumonia, otitis media and externa, and mild bronchiectasis. A BTK mutation mapping to a splicing site was confirmed by sequencing (Intron 7: 721+1 G-C). Drastically reduced but detectable *BTK* expression.

Patient 4 (Fig. 4F,G and 5E) was diagnosed with Bruton's agammaglobulinemia due to IgG, IgA and IgM below the detection limit and absence of peripheral B cells. The patient had suffered from recurring respiratory infections, including *Haemophilus influenzae*, bronchiectasis. The patient also developed an autoimmune enteropathy and ulcerating duodenitis treated by ileal resection.

MWS patient characteristics

All patients provided written informed consent for participation in the study. For further information refer to [1].

Patient 1 (Fig. 6D), female, aged 30, with confirmed p.E311K mutation. Complete response to anti-IL-1 therapy.

Patient 2 (Fig. 6D), male, aged 54, with confirmed p.E311K mutation. Complete response to anti-IL-1 therapy.

ACCEPTED MANUSCRIPT

292 **Patient 3** (Fig. 6A), male, aged 54, with confirmed p.E311K mutation. Complete response to anti-IL-1
293 therapy.

294 **Patient 4** (Fig. 6D), female, aged 5, with confirmed p.Q703K mutation. Currently not on anti-IL-1
295 therapy.

296 **Patient 5** (Fig. 6E), male, aged 46, confirmed p.R260W mutation. Complete response to anti-IL-1
297 therapy.

298 **Patient 6** (Fig. 6E), male, aged 60, with confirmed p.Val198Met mutation. Complete response to anti-
299 IL-1 therapy.

300

301 **Ibrutinib-treated patients**

302 All patients provided written informed consent for participation in the study.

303 **Patient 1** (Fig. 6G), male, aged 81. Primary diagnosis/indication for ibrutinib treatment: mantle cell
304 lymphoma (first diagnosed 09/2006). Secondary other disorders: Prostate Cancer, Hypertension,
305 Hyperthyroidism, chronic kidney disease. ibrutinib (Imbruvica©) dosage:560 mg/d orally. Time of last
306 administration before blood sampling (10:00 am): 8:00 am.

307 **Patient 2** (Fig. 6G), male, aged 80. Primary diagnosis/indication for Ibrutinib treatment: chronic
308 lymphocytic leukemia (first diagnosed 06/2008). Secondary other disorders: Hypertension,
309 hypogammaglobulinemia. Ibrutinib (Imbruvica©) dosage:420 mg/d orally. Time of last administration
310 before blood sampling (10:00 am): 8:00 am.

311 **Patient 3** (Fig. 6F), female, aged 86. Primary diagnosis/indication for ibrutinib treatment: chronic
312 lymphocytic leukemia (first diagnosed 05/2007). Secondary other disorders: atrial fibrillation.
313 ibrutinib (Imbruvica©) dosage: 280 mg/d orally. Time of last administration before blood sampling
314 (10:00 am): 8:00 am.

315 **Patient 4** (Fig. 6F), male, aged 64. Primary diagnosis/indication for ibrutinib treatment: mantle cell
316 lymphoma (first diagnosed 08/2008). Secondary other disorders: hypogammaglobulinaemia,
317 diabetes mellitus, polymyalgia rheumatica. ibrutinib (Imbruvica©) dosage: 560 mg/d orally. Time of
318 last administration before blood sampling (10:00 am): 8:00 am.

319 **Patient 5** (Fig. 6F), male, aged 60. Primary diagnosis/indication for ibrutinib treatment: chronic
320 lymphatic leukemia (first diagnosed 12/1999). Secondary other disorders: Secondary antibody
321 deficiency syndrome, history of autoimmune hemolysis with incomplete warm autoantibody,
322 Polyneuropathy in both feet, History of gram-negative sepsis at colitis with thickening of cecum and
323 colon ascendens, *E. coli* detection (BK), history of septic pneumonia with detection of *E. coli* (BK);
324 antibiosis with Tazobac Oesophageal varices grade III fundus varices grade I. Ibrutinib (Imbruvica©)
325 dosage: 420 mg/d orally. Time of last administration before blood sampling (10:00 am): between
326 6:00 and 9:00 am.

327 **Patient 6** (Fig. 6F), male, aged 87. Primary diagnosis/indication for ibrutinib treatment: chronic
328 lymphatic leukemia (first diagnosed 02/1994). Secondary other disorders: Pacemaker implantation,
329 sick sinus syndrome, brady-tachycardia, Permanent atrial fibrillation, currently on Apixaban, History
330 of duodenal ulcer, Forrest III hemorrhage, Choledocholithiasis History of stent implantation, post
331 interventional cholangiosepsis (E.Coli in pBK). Ibrutinib (Imbruvica©) dosage: 420 mg/d orally. Time
332 of last administration before blood sampling (10:00 am): between 6:00 and 9:00 am.

ACCEPTED MANUSCRIPT

333 **Supplemental References**

334 1. Rieber N, Gavrilov A, Hofer L, Singh A, Oz H, Endres T, et al. A functional inflammasome
335 activation assay differentiates patients with pathogenic NLRP3 mutations and symptomatic
336 patients with low penetrance variants. Clinical Immunology 2015; 157:56-64.
337 2. Verreck FA, de Boer T, Langenberg DM, Hoeve MA, Kramer M, Vaisberg E, et al. Human IL-23-
338 producing type 1 macrophages promote but IL-10-producing type 2 macrophages subvert
339 immunity to (myco)bacteria. Proc Natl Acad Sci U S A 2004; 101:4560-5.
340 3. Bartok E, Bauernfeind F, Khaminets MG, Jakobs C, Monks B, Fitzgerald KA, et al. iGLuc: a
341 luciferase-based inflammasome and protease activity reporter. Nat Methods 2013; 10:147-
342 54.
343 4. Franklin BS, Bossaller L, De Nardo D, Ratter JM, Stutz A, Engels G, et al. The adaptor ASC has
344 extracellular and 'prionoid' activities that propagate inflammation. Nat Immunol 2014;
345 15:727-37.
346 5. Stutz A, Horvath GL, Monks BG, Latz E. ASC speck formation as a readout for inflammasome
347 activation. Methods Mol Biol 2013; 1040:91-101.
348 6. Khan WN, Alt FW, Gerstein RM, Malynn BA, Larsson I, Rathbun G, et al. Defective B cell
349 development and function in Btk-deficient mice. Immunity 1995; 3:283-99.
350 7. Olsen JV, Macek B. High accuracy mass spectrometry in large-scale analysis of protein
351 phosphorylation. Methods Mol Biol 2009; 492:131-42.
352 8. Koch A, Krug K, Pengelley S, Macek B, Hauf S. Mitotic substrates of the kinase aurora with
353 roles in chromatin regulation identified through quantitative phosphoproteomics of fission
354 yeast. Sci Signal 2011; 4:rs6.
355 9. Schroeder MJ, Shabanowitz J, Schwartz JC, Hunt DF, Coon JJ. A neutral loss activation method
356 for improved phosphopeptide sequence analysis by quadrupole ion trap mass spectrometry.
357 Anal Chem 2004; 76:3590-8.
358 10. Cox J, Mann M. MaxQuant enables high peptide identification rates, individualized p.p.b.-
359 range mass accuracies and proteome-wide protein quantification. Nat Biotechnol 2008;
360 26:1367-72.
361 11. Cox J, Neuhauser N, Michalski A, Scheltema RA, Olsen JV, Mann M. Andromeda: a peptide
362 search engine integrated into the MaxQuant environment. J Proteome Res 2011; 10:1794-
363 805.
364 12. Elias JE, Gygi SP. Target-decoy search strategy for increased confidence in large-scale protein
365 identifications by mass spectrometry. Nat Methods 2007; 4:207-14.
366 13. Wang H, El Maadidi S, Fischer J, Grabski E, Dickhofer S, Klimosch S, et al. A frequent
367 hypofunctional IRAK2 variant is associated with reduced spontaneous hepatitis C virus
368 clearance. Hepatology 2015.
369 14. Carpenter AE, Jones TR, Lamprecht MR, Clarke C, Kang IH, Friman O, et al. CellProfiler: image
370 analysis software for identifying and quantifying cell phenotypes. Genome Biol 2006; 7:R100.
371 15. de Almeida L, Khare S, Misharin AV, Patel R, Ratsimandresy RA, Wallin MC, et al. The PYRIN
372 Domain-only Protein POP1 Inhibits Inflammasome Assembly and Ameliorates Inflammatory
373 Disease. Immunity 2015; 43:264-76.
374 16. Thurlow LR, Hanke ML, Fritz T, Angle A, Aldrich A, Williams SH, et al. Staphylococcus aureus
375 biofilms prevent macrophage phagocytosis and attenuate inflammation in vivo. J Immunol
376 2011; 186:6585-96.

Figure S1

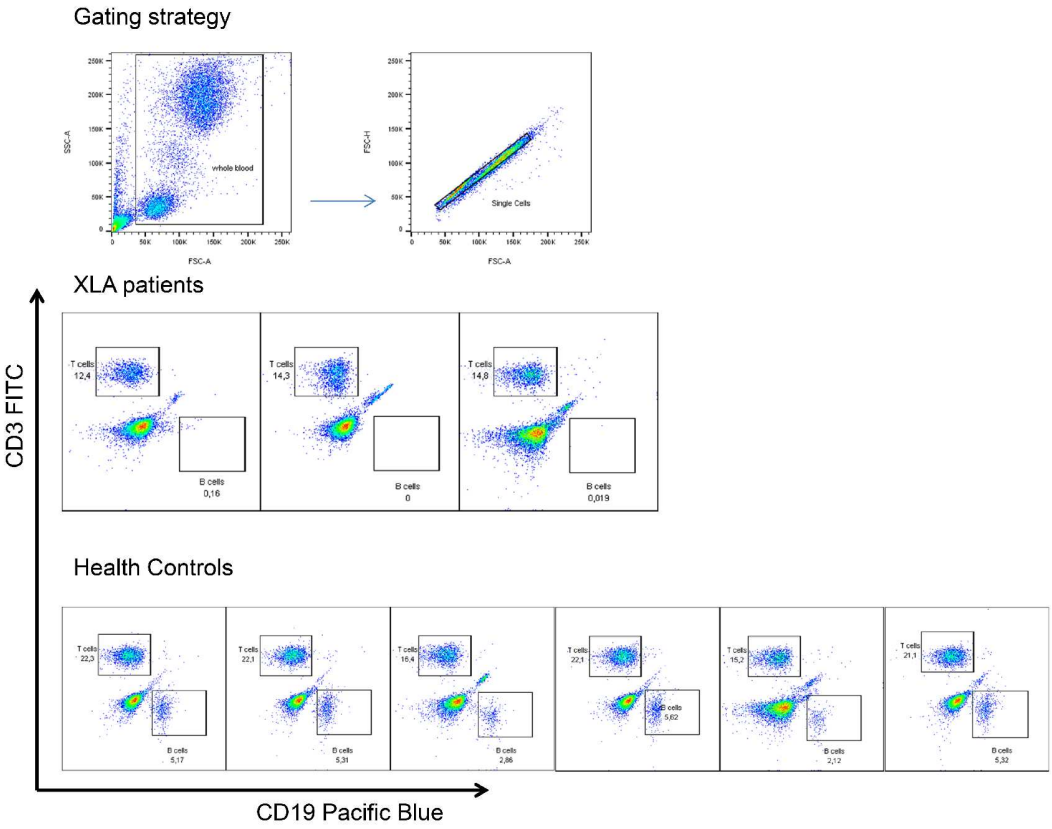

ACCEPTED

ACCEPTED MANUSCRIPT

Figure S2

A

z-stack confocal images of transfected HEK293T cells

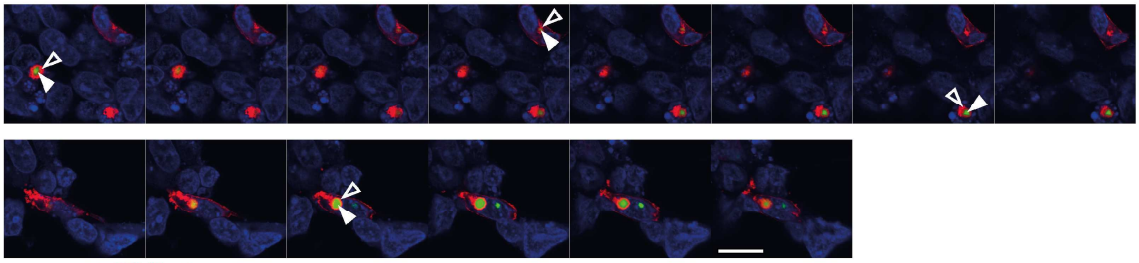

open arrowhead = BTK-HA outer sphere
filled arrowhead = ASC-GFP inner sphere
Blue pseudocolor = nuclei (To-pro-3)

B

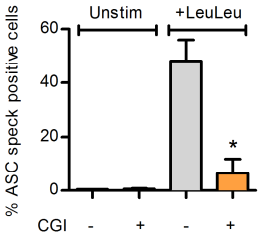

ACCEPTED MANUSCRIPT

Figure S3

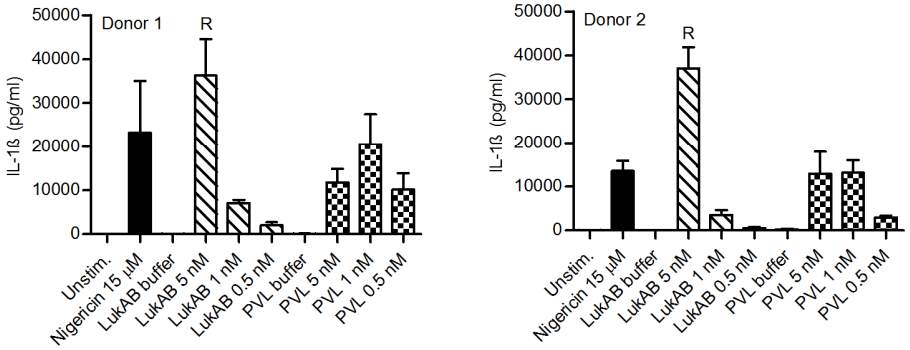

ACCEPTED MANUSCRIPT

Figure S4

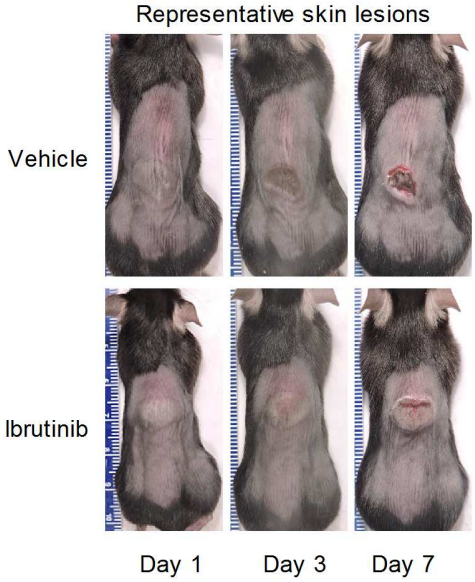

ACCEPTED MANUSCRIPT

Figure S5

A

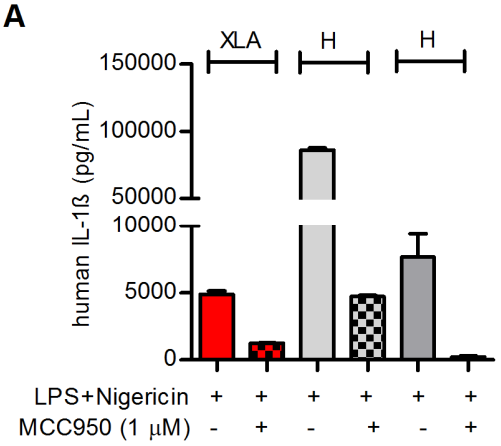

B

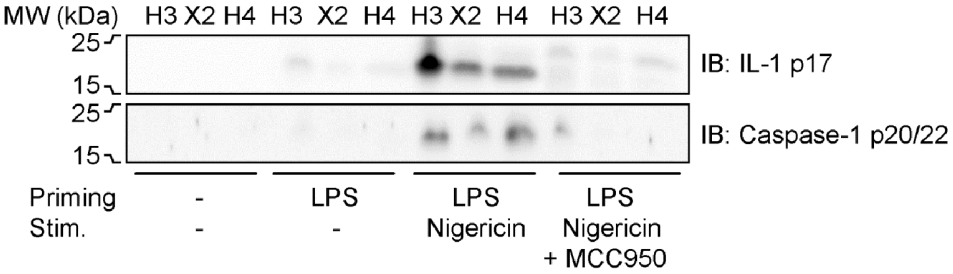

ACCEPTED MANUSCRIPT

Figure S6

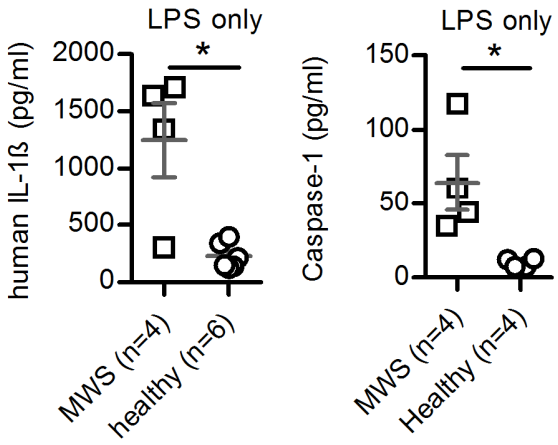

ACCEPTED MANUSCRIPT